

Alma Mater Studiorum Università di Bologna  
Archivio istituzionale della ricerca

Evolution of flood risk over large areas: Quantitative assessment for the Po river

This is the final peer-reviewed author's accepted manuscript (postprint) of the following publication:

*Published Version:*

Evolution of flood risk over large areas: Quantitative assessment for the Po river / Alessio, Domeneghetti; Francesca, Carisi; Attilio, Castellarin; Armando, Brath. - In: JOURNAL OF HYDROLOGY. - ISSN 0022-1694. - STAMPA. - 527:(2015), pp. 809-823. [10.1016/j.jhydrol.2015.05.043]

*Availability:*

This version is available at: <https://hdl.handle.net/11585/512767> since: 2015-12-20

*Published:*

DOI: <http://doi.org/10.1016/j.jhydrol.2015.05.043>

*Terms of use:*

Some rights reserved. The terms and conditions for the reuse of this version of the manuscript are specified in the publishing policy. For all terms of use and more information see the publisher's website.

This item was downloaded from IRIS Università di Bologna (<https://cris.unibo.it/>).  
When citing, please refer to the published version.

(Article begins on next page)

This is the final peer-reviewed accepted manuscript of:

Domeneghetti, Alessio, Francesca Carisi, Attilio Castellarin, and Armando Brath. "Evolution of Flood Risk over Large Areas: Quantitative Assessment for the Po River." *Journal of Hydrology* 527 (2015): 809-23.

The final published version is available online at:

<https://doi.org/10.1016/j.jhydrol.2015.05.043>

Rights / License:

The terms and conditions for the reuse of this version of the manuscript are specified in the publishing policy. For all terms of use and more information see the publisher's website.

This item was downloaded from IRIS Università di Bologna (<https://cris.unibo.it/>)

**When citing, please refer to the published version.**

1 **EVOLUTION OF FLOOD RISK OVER LARGE AREAS: QUANTITATIVE**  
2 **ASSESSMENT FOR THE PO RIVER**

3 Alessio Domeneghetti<sup>1\*</sup>, Francesca Carisi<sup>1</sup>, Attilio Castellarin<sup>1</sup>, Armando Brath<sup>1</sup>

4  
5 <sup>1</sup>DICAM – University of Bologna, School of Engineering, Viale del Risorgimento, 2, Bologna, Italy

6 \* Corresponding author: alessio.domeneghetti@unibo.it (tel. 0039 051 2093355)

7  
8 **ABSTRACT**

9 The worldwide increase of damages produced by floods during the last decades strengthens the  
10 common perception that flood risk is dramatically increasing due to a combination of different causes,  
11 among which climate change is often described as the major driver. Nevertheless, the scientific  
12 community is increasingly aware of the role of the anthropogenic pressures (e.g. steady expansion of  
13 urban and industrial areas in dyke-protected floodplains) that may strongly impact the flood risk in a  
14 given area by increasing potential flood damages and losses (i.e. so called “levee effect”). The scientific  
15 literature on quantitative assessments of the “levee-effect” or robust methodological tools for  
16 performing such assessments is still sparse. We refer to the dyke-protected floodplains of the middle  
17 and lower portion of River Po (Northern Italy), a broad geographical area (~46 000 km<sup>2</sup>) with two  
18 specific research questions in mind: (i) has the flood risk increased over the last half century? And, if  
19 so, (ii) what are the main drivers of this change? First, we assess the flood-hazard evolution by  
20 analysing three long series of daily streamflow available at different gauging stations. Secondly, we  
21 quantitatively assess the temporal variability of the flood exposure and risk by looking at the evolution  
22 in time of anthropogenic pressures (i.e. land-use and demographic dynamics observed from 1950s).  
23 To this aim, we propose graphical tools (i.e. Hypsometric Vulnerability Curves-HVCs) that are suitable  
24 for assessing vulnerability to floods over large geographical areas. Our study highlights the absence of

25 statistically significant trends in annual statistics of the observed streamflow series and a stable  
26 population density within the dike-protected flood-prone area. Nevertheless, the proposed flood-  
27 vulnerability indexes show a significant increase of the exposure to floods in residential settlements,  
28 which has doubled since the 1950s.

29

30 **Key Words:** “Levee effect”; exposure to floods; flood hazard and risk assessment; Po river;  
31 Hypsometric vulnerability curve.

32

## 33 **1 Introduction**

### 34 **1.1 Flood-risk change: evidences, main drivers and open problems**

35 Freshwater flooding (such as river floods, flash floods, urban inundation due to drainage  
36 problems, etc.) is the most impacting natural disaster in terms of number of people affected and  
37 economic damages (see e.g. EM-DAT; <http://www.emdat.be/>). Referring to the EM-DAT data-set,  
38 Jonkman (2005) analyzed the disasters occurred over the time period 1975-2001 and showed that  
39 floods are the most frequently recorded natural hazards occurring world-wide and, even though  
40 droughts and earthquakes might be more significant in terms of loss of life, floods are the events that  
41 most directly hit the largest number of people (around 2.2 billion of people between 1975-2001).

42 The common perception of an increasing frequency of floods and inundation phenomena during  
43 the last decades is often supported by a growing concern on climate change (e.g. European  
44 Environmental Agency-EEA, 2005; Wilby et al., 2008). In fact, some studies in the literature (e.g. IPCC,  
45 2013, and Stern Review, 2007) seem to indicate that flood damages are expected to increase in the  
46 near future as a consequence of a global climate change (see e.g. Hall et al., 2005; de Moel et al.,  
47 2011a). Climate change has increased worldwide the interest on understanding the interaction  
48 between human activities and the hydrological cycle. The scientific literature provides numerous  
49 studies that analyze long time series of hydrological variables (such as rainfall, river discharges,

50 temperature, etc.) to investigate the presence of significant trends in different contexts and at different  
51 scales (Petrow and Merz, 2009; Hamed, 2008; Vorogushyn and Merz, 2013; Villarini et al., 2011).  
52 However, it is worth noting that flood damages are the result of a complex system of factors that  
53 influence the overall dynamics and impacts of flood events (see e.g. Merz et al., 2010; Elmer et al.,  
54 2012), and climate variability is only one component.

55 Many studies highlighted that the economic and social development in flood-prone areas are key  
56 elements for a correct interpretation of the increase of flood losses observed during last decades (see  
57 e.g. Ludy and Kondolf, 2012; Di Baldassarre et al., 2013, and references therein). For instance,  
58 considering the flood-related costs recorded in Europe over the time period 1970-2006, Barredo  
59 (2009) shows that there is no evidence of a positive trend on normalized damages; that is, a large  
60 portion of the growth of nominal losses associated with floods can be explained by the evolution of  
61 exposure to floods and wealth in floodplains. Similar results have been found looking at the damages  
62 and costs associated with hurricanes in United States between 1900 and 2005 (see Pielke and  
63 Landsea, 1998, and Pielke et al., 2008) and to globally observed disasters associated with water (see  
64 Neumayer and Barthel, 2011; Barredo, 2009). All these studies show that there are no clear evidences  
65 of an increasing trend in the normalized economic damages, even though the difficulties in considering  
66 the overall mitigation measures enforced by authorities or individuals prevent one to infer that  
67 historical data do not show a clear positive trend in the frequency and/or intensity of weather-related  
68 natural disasters (Neumayer and Barthel; 2011). Thus, even though historical data do not provide  
69 incontestable proofs of the loss increase due to climate change, caution is needed in the evaluation of  
70 the overall effects of climate change and the precautionary principle should, in any case, support the  
71 reduction of possible human impacts (Neumayer and Barthel; 2011).

72 These considerations are supported by investigations performed on flood risk projections over  
73 the future decades in different areas and contexts of the world (see e.g. Elmer et al., 2012; De Moel et  
74 al., 2011a; Bouwer et al., 2010). These studies highlight how land-use changes and economic  
75 development of hazard-prone areas (i.e. flood-risk exposure) may have an effect on the increase of  
76 flood losses that is comparable to, if not higher than, what is commonly associated with the expected

77 climate change. For instance, population growth and the increase of exposed wealth in flood-prone  
78 areas may significantly increase potential damages during flood events, and may end up being the  
79 main factors controlling the increase in recorded damages (Bouwer et al., 2010).

80 These considerations strengthen the interpretation of floodplains as complex human-water  
81 systems, in which the interactions between the two elements is so strong that the current floodplain  
82 configuration is actually the result of the interplay between human activities (such as flood controls,  
83 land-use changes and other measures that may affect the frequency and magnitude of flooding events)  
84 and hydrological dynamics (e.g. the frequency and severity of floods may constrain the development of  
85 human settlements) (Di Baldassarre et al., 2013; Schultz and Elliott, 2012).

86 A typical expression of this strong interaction is the so-called “levee effect” (Tobin, 1995), also  
87 named “levee paradox” or “call-effect”, according to which the flood-prone areas protected by a levee  
88 system attract and encourage new human settlements. The increase of the overall vulnerability of the  
89 areas may potentially result in higher damage in case of extreme flood events that cannot be  
90 restrained by the existing levee system, or in case of levee-system failures (i.e. what is usually  
91 identified as “residual flood risk”; see e.g. Castellarin et al., 2011a; Di Baldassarre et al., 2009).  
92 Investigating a specific case study in California, Ludy and Kondolf (2012) clearly point out that the  
93 presence of a levee system changes the perception of the flood likelihood in people living in the dyke-  
94 protected areas, which are perceived as completely safe from inundations. This feeling ends up  
95 increasing the vulnerability of floodplains, even in areas that were already affected by inundations,  
96 where the demographic and economic growth experienced after the inundation, due to the  
97 enhancement of the levee system, led to a well-being condition that is higher than before the  
98 inundation (Schultz and Elliott, 2012).

99 All these considerations underline the necessity to analyze flood risk and its evolution in time by  
100 means of holistic approaches, which take into account the interaction between social and hydrological  
101 factors characterizing a large geographical areas. A better understanding of the interplay between  
102 these elements represents a fundamental piece of information for the identification of robust large

103 scale flood-risk mitigation strategies and the definition of viable development plans for flood-prone  
104 areas. However, although the “levee effect” phenomenon (Tobin, 1995; also named “call-effect”) is  
105 frequently mentioned, the literature on its objective quantification is still very sparse and many  
106 studies refer to estimates evaluated on each case study (see e.g. Merz et al., 2009).

107

## 108 **1.2 Study aims**

109 Our study focuses on the middle-lower portion of the Po river and aims at analyzing the evolution  
110 during the last half century of residual flood risk in the dyke-protected floodplains. The hydrological  
111 behaviour of the Po river basin has been investigated in several previous studies (see e.g., Zanchettini  
112 et al., 2008; Montanari, 2012 and references therein), nevertheless the scientific literature does not  
113 report any comprehensive analysis of the historical flood-risk dynamics for the entire middle-lower  
114 portion of the Po river nor of the influence on this dynamics of the main controlling factors (e.g. human  
115 activities that developed during last decades, climatic variability, etc.). In particular, we address the  
116 investigation of the evolution in time of flood hazard and exposure to floods, being the flood risk of a  
117 given area the combination of the probability of inundation (e.g. flood hazard) and of the expected  
118 adverse consequences (i.e. flood exposure and damage susceptibility of the flood-prone areas, see e.g.  
119 EXCIMAP, 2007).

120 First, we analyse long streamflow series available at different gauging stations located along the  
121 study reach, statistically falsifying the hypothesis of changes in flood-hazard during the last half  
122 century similarly to what have been shown for other regions of the world (see e.g. Kundzewicz et al.,  
123 2005; Svensson et al., 2005). Second, we propose a simplified and robust approach for the  
124 quantification of flood-risk dynamics associated with the evolution of exposure to floods. Third, we  
125 quantitatively assess the evolution of flood risk in the dyke-protected floodplain of the study reach,  
126 assessing the anthropogenic pressure by referring to land-use (i.e. focussing on residential areas) and  
127 demographic dynamics observed from 1950s.

128 In particular, since the study area is protected against 200-year flood events (Po River Basin  
129 Authority-Adb-Po, 1999), we focus on the residual risk dynamics, thus referring to a specific low-  
130 frequency flooding scenario for which the protection measures are insufficient (see Section 5.1 for  
131 more details). We propose simplified flood-vulnerability indexes based on land-use and topographic  
132 information that are particularly suitable for large spatial scales, which we use to (1) assess the  
133 importance of the different elements contributing to the definition of flood risk and, (2) represent the  
134 evolution in time of flood exposure and residual flood risk in the flood-prone area of interest. Finally,  
135 we quantitatively assess whether during the last half-century the study area experienced the so called  
136 levee-effect, and to what degree it impacted the residual flood risk.

137 Our manuscript is structured as follows: Section 2 illustrates the study area and data used for the  
138 analysis; Section 3 investigates the flood-hazard evolution during the last half century; Section 4  
139 describes the methodologies used for investigating the flood-exposure evolution; Section 5 presents  
140 the selected inundation scenario and methodologies used for the large-scale estimation of flood  
141 damages; Section 6 reports the results of the study. Finally, Section 7 reports a comprehensive  
142 discussion of the results.

## 143 **2 Study area and available data**

144 The study area consists of the alluvial plain of the Po river, the longest Italian river that flows  
145 eastward through the Northern part of Italy for about 650 km. With a total extent of about 71 000 km<sup>2</sup>  
146 the Po river basin is the wider Italian catchment and covers a large portion of the Emilia-Romagna,  
147 Lombardy, Piedmont, Aosta Valley and Veneto (see Figure 1). This area, in particular the Alpine  
148 foothills and flat portion of the basin, represents one of the most developed and populated area of  
149 Italy: more than 45% of employed Italians live here producing almost 40% of the total Italian Gross  
150 Domestic Product (GDP) (Po River Basin Authority, AdB-Po, 2006; [www.adbpo.it](http://www.adbpo.it)).

151

152

*Figure 1*



153

154 The middle-lower stretch of the Po river flows across a flat and fertile alluvial area, named  
155 Pianura Padana (overall extent of around 46 000 km<sup>2</sup>), where the flood-prone areas that are closer to  
156 the Po river, or its major tributaries, are protected from frequent inundations by means of a complex  
157 system of embankments and other hydraulic structures (e.g. pumping stations, sluice gates, etc.) that  
158 are monitored and maintained by the Interregional Agency of the Po River (AIPO;  
159 [www.agenziainterregionalepo.it](http://www.agenziainterregionalepo.it)) and by the Po River Basin Authority (AdB-Po).

160 The current embankment system represents the result of the people struggle during the last  
161 centuries to prevent the loss of their properties and assets due to floods. From 1705 to 1951 Pianura  
162 Padana was hit by 18 major floods with 225 embankment failures along the main river or its major  
163 tributaries (Govi and Turitto, 2000). In the inundations aftermath the embankment system was  
164 continuously strengthened and extended, increasing from a total length of about 1 500 km on 1878, to  
165 more than 2 900 km after the flood event of the 1951, when the lower stretch of the Po river  
166 experienced a catastrophic flood event that caused a large inundation (~1 080 km<sup>2</sup>; see Masoero et al.,  
167 2013) and severe damages (e.g., 100 victims, 900 houses seriously damaged and around 200 000  
168 refugees; Amadio et al., 2013).

169 Castellarin et al. (2011a) and Di Baldassarre et al. (2009) clearly emphasized this aspect showing  
170 the evolution in time of the overall length of the embankment system along the Po river and major  
171 tributaries between 1800 and '50-'60s and the associated increasing trend in the sequence of annual  
172 maximum water level at the Pontelagoscuro streamgauge (see Figure 1), located at the catchment  
173 outlet (see also Heine and Pinter, 2012). During the last decades (i.e. from 60's) the actions of  
174 adjustment of the levee system along the lower portion of the river mainly focused on the  
175 strengthening of the existing embankment, while further embankment widening and raising were  
176 implemented after the flood event of October 2000 (see Coratza, 2005; Castellarin et al., 2011a). The  
177 current river configuration is reported in Figure 1 (box), which shows the main river stretch, the main  
178 embankment system, as well as the area that can potentially be flooded in case of catastrophic flood

179 events (blue polygons). This area, named “Fascia-C” (literally C-Buffer, which we consistently use in  
180 the remainder), is characterized by an overall extent of  $\sim 6\ 100\ \text{km}^2$  and was identified by the Po River  
181 Basin Authority (AdB-Po, 1999) as the envelope of all areas associated with a non-negligible residual  
182 risk of being flooded, that is areas that can be flooded in case of sudden and unpredictable failures of  
183 the embankment system (i.e. breaches in the embankments along the main river or tributaries that are  
184 triggered e.g. by piping during major floods) or in case of flood event with a recurrence period higher  
185 than the one adopted for the design of the embankments (i.e.  $\sim 200$  year, AdB-Po, 1999). The box on  
186 Figure 1 shows the C-Buffer area divided into different compartments defined referring to the layout  
187 of natural and man-made structures (e.g. embankments for the Po river and its main tributaries, rivers,  
188 roads, etc.; see also Castellarin et al., 2011b).

189 Despite the existence of a non-negligible residual risk in the C-Buffer (i.e. the levee failure  
190 occurred in 1951 is an evidence of the residual risk that still exists in the flood-prone area), the feeling  
191 of safety ensured by the embankment system attracted human settlements and the area itself went  
192 through a significant economic development during the 20th century. In the light of these  
193 considerations, together with the availability of historical land-use information (see Section 2.1 for  
194 details), we investigate the factors that driven the evolution of the residual flood risk in the flood-  
195 prone areas during last decades, focusing in particular in the period that goes from 1950s up to now.

196

## 197 **2.1 Available data**

198 We refer to data of various type collected from different sources. The following list briefly  
199 summarizes the data set used for the analyses, while further information on the actual utilization of  
200 these data are provided in Sections 3, 4 and 5:

- 201 - *Streamflow data*: Table 1 summarizes the characteristics of daily streamflow series recorded  
202 at streamgauges of Moncalieri, Piacenza and Pontelagoscuro (see Figure 1), with lengths of 42,  
203 85 and 89 years, respectively.

- 204 - *Land-use maps*: land-use maps are available for the C-Buffer and different time periods from  
205 cartographic offices of Emilia-Romagna and Lombardy administrative districts (see Figure 1).  
206 In particular, land-use information is retrieved from aerial imagery available for 1954 (G.A.I-  
207 Gruppo Aereo Italiano and WWS flights) and 2008 (AGEA-2008), with a resolution of about  
208 150 m and 75 m, respectively, and classified referring to the standardized classes aggregation  
209 adopted by the CORINE (COoRdinated INformation on the Environment) project (EEA, 2009).
- 210 - *Demographic dynamics*: number of inhabitants available throughout Italy since 1861. The  
211 Italian National Statistical Institute (ISTAT; <http://www.istat.it>) provides information on the  
212 population dynamics with ten-year frequency at each census sections.
- 213 - *Assets economic values*: economical values of residential buildings in the alluvial area. The  
214 Italian Revenue Agency (Agenzia delle Entrate (AE); <http://www.agenziaentrate.gov.it>)  
215 provides the open-market values for different assets, taking into account different classes for  
216 residential and industrial buildings and the overall economic well-being of the region (see  
217 Section 5.2 for more details).
- 218 - *Topographic information*: topography of the study area is retrieved from TINITALY/01  
219 (Tarquini et al., 2007). Created by using heterogeneous elevation datasets (i.e. contour lines,  
220 elevation points, etc.), TINITALY/01 represents the most accurate Digital Elevation Model  
221 (DEM) covering Italy. It is characterized by a horizontal resolution of 10 m and a vertical  
222 accuracy (i.e. root mean square errors ranging from 0.8 to 6 m) higher relative to other global  
223 DEMs (i.e. SRTM, ASTER; see Tarquini et al., 2012).

224

### 225 **3 Flood-hazard evolution – trend detection in streamflow series**

#### 226 **3.1 Methods**

227 Many studies investigated the streamflow regime of the Po river (see e.g., Visentini, 1953; Piccoli,  
228 1976; Marchi, 1994). Zanchettini et al. (2008) analyzed the long-term daily streamflow variability at

229 Pontelagoscuro (see Figure 1) by referring to a time series longer than 200 years, in which some daily  
230 streamflow values were re-constructed from historical information on water surface. The analysis  
231 highlighted an increase in the streamflow values observed at the streamgauge of Pontelagoscuro  
232 during last decades, concluding that this increase could be mainly attributed to the massive  
233 embankment works implemented along the river network during previous decades, rather than to  
234 climate changes. The authors also pointed out the existence of perturbation periods (mainly associated  
235 with droughts) lasting for several years. More recently, Montanari (2012) reached similar conclusions  
236 by investigating the variability of daily streamflows observed along the Po river and some its major  
237 tributaries. The study highlighted the presence of local perturbations (i.e. periods characterized by  
238 water scarcity, or water abundance), whose memory lasts for long periods of time (i.e. several years),  
239 which can be associated with the size of the drainage area. Even though this evidence suggests the  
240 presence of long-term persistence that would be worth investigating, the research of trend interested  
241 only the gauged section of Pontelagoscuro and was made by means of a linear regression application.

242 In this study, we further analyse the variability of the daily streamflow regime of the Po river by  
243 testing for trends the daily streamflow series collected at three gauging sections along the main  
244 stream: Moncalieri, Piacenza and Pontelagoscuro (see also Figure 1 and Table 1). The streamgauges  
245 are located along the same river and therefore the observed daily streamflow series are necessarily  
246 statistically correlated to each other, which is likely to result in similar outcomes of statistical testing  
247 (see Douglas et al., 2000). Nevertheless, we considered all three series since they refer to rather  
248 different drainage areas and periods of time (see Table 1 and Figure 1). In particular, we adopted the  
249 non-parametric Mann-Kendall (MK) test (Mann, 1945; Kendall, 1975), that is one of the most robust  
250 trend detection method applied in many studies to different hydrological variables (see for example  
251 Yu and Wang, 2004, and references therein) and spatial scales (see e.g. Douglas et al., 2000; Hamed,  
252 2008; Villarini et al., 2011). The MK test analyses the ranks of the observations rather than their actual  
253 values, it is non-parametric (distribution-free) and less sensitive to outliers than other parametric  
254 approaches, therefore the MK test appears to be particularly suitable for detecting statistically  
255 significant trends in hydrological time series (see Yue et al., 2002, Petrow et al., 2009). However, the

256 presence of serial correlation among the daily streamflow data may impact the power of MK test (von  
257 Storch and Cannon, 1995). To overcome this problem we applied the trend free pre-whitening (TFPW)  
258 procedure to the study series; TFPW removes serial correlation from time series, and hence it  
259 eliminates the effect of serial correlation on the MK test (see Yue et al., 2002, for details). In particular,  
260 we perform a two-sided trend test at 5% significance level through the MK-TFPW procedure on the  
261 sequences of annual maxima (AMS), mean (MEAN) and standard deviation (SD) of daily streamflows.

262 *Table 1*

263

### 264 **3.2 Results and Discussion on flood-hazard evolution**

265 Figure 2 shows the annual sequences of maxima (AMS), mean (MEAN) and standard deviation  
266 (SD) of daily streamflows at Moncalieri, Piacenza and Pontelagoscuro, along with the related linear  
267 regression lines fitted over the observation period. Table 2 reports the results of the Mann-Kendall  
268 (MK) trend analysis test, listing Sen's slope value,  $\beta$ , test  $p$ -value, and increase/decrease of the  
269 statistics over the observation period,  $\Delta$ .

270 Figure 2 clearly highlights the absence of significant and consistent long-term trends on the daily  
271 streamflow statistics (i.e. AMS, MEAN, SD) computed for the three streamgauges over the  
272 corresponding observation periods. Considering Moncalieri cross-section, Sen's slopes,  $\beta$ , appear to be  
273 limited for all considered statistics, pointing out a small increase in the annual maxima and mean  
274 discharge values ( $\beta$  equal to 2.09 and 0.31 m<sup>3</sup>/s/year, respectively; see Table 2), while the river daily  
275 streamflow variability (i.e. SD) is almost constant over the period ( $\beta$ =-0.02 m<sup>3</sup>/s/year).  $p$ -values  
276 reported for Moncalieri indicate the absence of statistically significant long-term trends at 5% level.  
277 Similar results are observed at Piacenza, where MEAN and SD do not show significant changes over  
278 the observation period, even though AMS is associated with a limited increase ( $\beta$  equal to 2.02  
279 m<sup>3</sup>/s/year), which is consistent with the one observed for Moncalieri. The slight increase of annual  
280 maximum daily discharges in the upstream cross-sections of Moncalieri and Piacenza (see Figure 1) is  
281 confirmed at Pontelagoscuro, where this feature appears to be emphasized (see Figure 2 and Table 2).

282 AMS series at Pontelagoscuro is associated with a slope  $\beta$  of 13.2 m<sup>3</sup>/s/year, with an overall increase  
283 of about 1178 m<sup>3</sup>/s for 90-year observation period; although not negligible, this trend is not significant  
284 from a statistical viewpoint (p-value = 0.106).

285 Furthermore, concerning the non-significant positive trend associated with the last 90 years of  
286 observations, it is worth highlighting that the same analysis repeated for the data observed after 1950  
287 results in a statistically non-significant negative trend of -2.73 m<sup>3</sup>/s/year. Finally, Pontelagoscuro  
288 MEAN sequence does not evidence any change during the observation period, while SD shows an  
289 overall increase of about 225 m<sup>3</sup>/s, which is significant at the 5% level (see Table 2).

290 The extended analysis of historical stream flow series carried out in our work confirms the  
291 findings of previous studies (e.g. Montanari 2012; Zanchettini et al., 2008) and highlights the absence  
292 of statistically significant trends on streamflow series along the overall river reach (see Figure 2). The  
293 impact of the flood-hazard variability in the assessment of the residual flood risk dynamics during the  
294 last half century appears to be practically negligible and statistically not significant, making reasonable  
295 the hypothesis of stationarity of the streamflows data set. On the basis of these considerations the  
296 likelihood of extreme flood events responsible for the residual flood risk in the area of interest (such  
297 as flood events with return period higher than 200 years) can be considered not significantly changed  
298 during the last half century.

299 *Table 2 – Figure 2*

300

## 301 **4 Evolution of exposure to floods: simplified tools for large-scale applications**

### 302 **4.1 Land-use dynamics**

303 We investigate the land-use evolution in the Po river basin focusing in particular on Emilia-  
304 Romagna and Lombardy administrative districts (see Figure 1), which cover entirely the C-Buffer (i.e.  
305 the floodable area in case of the Tr-500 flood event; see box in Figure 1). Our analysis considers land-  
306 use maps available for 1954 and 2008 (see Section 2.1). The maps were constructed on the basis of

307 historical aerial photographs with different spatial resolution (150 m and 75 m for the 1954 and 2008  
308 maps, respectively), however the land-use classifications adopted in both cases are consistent and  
309 enable one to compare the two time periods. The land cover data in both maps use a hierarchical  
310 structure similar to the one adopted by the CORINE project (EEA, 2009), in which different soil-uses  
311 are organized by means of several levels of aggregation. In this study the evaluation of the flood  
312 exposure evolution is performed referring to urban and residential areas only. Table 3 reports the land  
313 cover categories used for the different maps adopting the CORINE classification as reference.

314 *Table 3*

315 We evaluate the expansion of urban and residential areas by referring to two different spatial  
316 scales. First we consider a local scale by referring to C-Buffer compartments only (see Figure 1).  
317 Second, we evaluate the land-use evolution at a larger scale (i.e. regional analysis), comparing the  
318 overall extension of urban areas in 1954 and 2008 in Emilia-Romagna and Lombardy districts. Results  
319 obtained for the local (C-Buffer) and regional (large-scale) analyses can then be compared to gain a  
320 deeper understanding of the evolution of exposure to floods, providing interesting insights to foster  
321 the discussion on the effectiveness of the “levee-effect” (or “call effect”) on the floodplains areas (see  
322 Sections 6 and 7).

323 We use the land-use maps described above to derive a large-scale assessment of the exposure to  
324 floods in the C-Buffer. In particular, we combined the land-use class of interest (i.e. urban settlements)  
325 of each compartment with the digital description of the topography (i.e. 10 m DEM; see Section 2.1) to  
326 retrieve a simplified altimetric description of urban and residential areas through a so-called  
327 hypsometric curve, which we named Hypsometric Vulnerability Curve (HVC). The hypsometric curve  
328 of a given area reports on the x-axis the percentage (or the portion) of area characterized by elevations  
329 lower than the value reported on the y-axis. HVCs of each compartment of the C-Buffer combine land-  
330 use information with information on elevation retrieved from the 10 m DEM. Zhang et al. (2011) firstly  
331 proposed the use of hypsometric curves in the Florida Keys for the evaluation of the impact of  
332 different scenarios of sea level rise on human population and real estate property.

333

334

*Figure 3*

335

336 As an example, Figure 3 reports a schematic representation of the HVC defined for a specific  
337 compartment and land-use class. We construct the urban and residential areas HVCs for each  
338 compartment for 1954 and 2008 in a GIS (Geographic Information System) environment. HVCs  
339 represent a valuable tool for a preliminary assessment of the exposure to floods of each compartment,  
340 and, when one can construct curves relative to different time periods as in our case, these curves can  
341 be particularly useful for characterizing the dynamics of urban areas over a given historical period  
342 (e.g. in the dike-protected floodplain of the Po river over the last half century). The schematic  
343 representation of Figure 3 illustrates HVC and the information that can be retrieved from such a curve.  
344 For instance, the HVC graphically represents the altimetric characteristics of a specific land-use class  
345 in a given compartment (e.g. residential settlements), and HVCs of different periods enable one to  
346 assess how and where (i.e. closer or farther to the river) a specific land-use class developed over time  
347 (see Section 6.1 and Figure 7 for details). Furthermore, assuming the dashed line of Figure 3 as a  
348 hypothetical inundation level, its intersection with the HVC identifies the extent of the affected area  
349 and may be particularly useful for a prompt assessment of flood damages (see Section 5.2 for details).

350

## 351 **4.2 Population dynamics**

352 The number of people living in flood-prone areas represents a fundamental element for the  
353 evaluation of the exposure to floods and is a key factor of the “levee effect” phenomenon (see e.g. Di  
354 Baldassarre et al., 2010, 2013; Barredo, 2009). Accordingly, we analyze the population dynamics in the  
355 Po river basin, assessing if the strengthening of the levee system carried out during last century (see  
356 Section 2 and also Di Baldassarre et al., 2009, and Castellarin et al., 2011a) is associated with any  
357 population growth in the flood-prone areas in spite of the residual flood risk. In particular, we evaluate  
358 the population dynamics from 1861 to 2011 considering the number of inhabitants recorded by the



359 Italian National Statistical Institute (ISTAT) (census data are provided with a 10-year frequency) and  
360 provided for each Italian municipality. Once collected, the population data have been gathered  
361 together distinguishing between Emilia-Romagna and Lombardy regions and all of the compartments  
362 of the C-Buffer (see Figure 1).

363 Given the extent of urban areas and the overall number of inhabitants living in a specific  
364 municipality within a C-Buffer compartment we estimate the population density under the hypothesis  
365 of a uniform distribution over the urban extent. The population density of a specific compartment is  
366 calculated as the weighted average among different municipalities, weighting that data proportionally  
367 to extent of urban areas. Then, we derive the Hypsometric Inhabitant Curves (HICs) for 1954 and  
368 2008 by combining the average population density with the altimetry of the urban area in a given  
369 compartment (see the procedure adopted for the HVC construction; Figure 3). HICs are curves that  
370 report the overall number of inhabitants living in a compartment below a given elevation: they  
371 integrate information on the number of people living in a specific compartment with the overall extent  
372 of urban areas, obtained from land use maps, and elevation retrieved from a DEM of the area of  
373 interest. The curves may represent useful tools for a preliminary evaluation of the exposure to floods  
374 of a specific area. For instance, HICs may enable one to estimate the number of people that could be  
375 affected by a given inundation scenario over a floodplain area; alternatively, HICs constructed for a  
376 given inundation scenario and floodplain compartment by considering census data and land-use maps  
377 for different years may effectively summarize the impacts of demographic dynamics on flood risk.

378

## 379 **5 Damage calculation for urban areas**

380 Flood risk management recently shifted its main focus from flood hazard (i.e. hazard reduction) to  
381 a risk-based view (i.e. risk reduction) (see e.g. Vis et al., 2003; Merz et al., 2010; De Moel et al., 2012).  
382 This approach considers the interplay between hydrological and socio-economic factors and the  
383 calculation of the expected flood damage represents a fundamental piece of information for the overall  
384 flood-risk mitigation process. The evaluation of the overall costs of natural hazards, such as flood

385 events, is a challenging task due to the variety of damage types that may be directly or indirectly  
386 related to the hazard. Meyer et al. (2013) recently summarize these costs distinguishing four different  
387 categories identified in relation to their nature and to the methodologies adopted for their assessment:  
388 direct and indirect costs, business interruption costs, and intangible costs. Considering flood events,  
389 direct costs represent the damages occurred to properties (e.g. buildings, stocks, cars, infrastructure,  
390 etc.) physically hit by the flood. Business interruption costs result from the interruption of the  
391 economic activities in the flooded areas, for example because of inaccessibility or because of the  
392 destruction of the working instruments (see Meyer et al., 2013). Indirect costs summarize all the  
393 economic losses that can be related to direct and indirect (e.g. business interruption) damages,  
394 occurred both inside or outside the affected area, even considering the effects on a broad timeframe  
395 after the event (see Carrera et al., 2015 for more details). Finally, intangible costs consider the impact  
396 on services, goods or human beings which have not a market value and for which the damage  
397 estimation in monetary terms is not trivial, if not impossible (e.g. health and environmental impacts,  
398 damages to cultural heritage, etc.; Meyer et al., 2013; Markantonis et al., 2012).

399 Concerning the estimation of different types of flood losses the literature provides a series of  
400 methodologies of various complexity based on different type of data and assumptions, and suitable for  
401 different scales of application (see Meyer et al., 2013, for a comprehensive review of these  
402 approaches). Traditionally, the flood damage assessments mainly refer to direct losses in view of the  
403 greater ease with which they can be estimated. In particular, the scientific community proposes  
404 simplified damage models that estimate the expected direct flood damages by means of depth-damage  
405 functions (also named susceptibility functions), where the economic damage of a specific element (e.g.  
406 a building) is a non-decreasing function of the water depth, which is sometimes integrated with some  
407 other hazard factors (i.e. flow velocity, duration, pollution, etc.; see Jongman et al., 2012). More  
408 recently, sophisticated multi-parameter models have been proposed for a local estimation of losses in  
409 private households and companies (e.g. FLEMO; see Kreibich et al., 2010; Elmer et al., 2010). Even  
410 though the former approach is less accurate and associated with a larger degree of uncertainty (see  
411 e.g. Apel et al., 2008; De Moel et al., 2011b), in the light of the large spatial scale of interest (i.e. overall

412 C-Buffer area) we estimate the expected flood damage referring to a simplified approach based on the  
413 joint use of a depth-damage curve and the previously defined HVCs.

414 Differently from previous applications, where hypsometric curves were used only for identifying  
415 the extent and amount of affected properties (see Zhang et al., 2011 for sea level rise scenarios), we  
416 propose an original application of HVCs in combination with a given inundation scenario and specific  
417 depth-damage curves (e.g. accurately identified for a specific land-use or buildings type, see Section  
418 5.2 for a detailed description about flood damage estimation) that enables the user to calculate the  
419 flood losses. We focus on direct damages (i.e. direct tangible damage) for residential building, while we  
420 neglect all other costs in this preliminary application.

421

## 422 **5.1 Inundation scenario**

423 For the evaluation of the flood hazard we refer to the inundation scenario generated by the  
424 numerical model developed by Castellarin et al. (2011b) whom implemented a quasi-two-dimensional  
425 (quasi-2D) model (Willems et al., 2002) for the Po river stretch considered herein (from Isola S.  
426 Antonio to Pontelagoscuro, ~350 km; see Figure 1). The model describes the main river reach by  
427 means of cross-sections retrieved from a detailed digital elevation model (LiDAR, with a spatial  
428 resolution of 2 m), while all dike-protected floodplains are represented as storage areas connected to  
429 each other and/or the main channel by means of weirs mimicking the system of minor levees.  
430 Adopting a similar modeling strategy, all C-Buffer compartments are represented as storage areas and  
431 connected to the main river, or dike-protected floodplains, by means of lateral structures that  
432 reproduce the main embankment crests. Volume-level curves regulate the hydraulic behavior of all  
433 storage areas, and, in case of inundation of a dyke-protected floodplain or C-Buffer compartment, the  
434 simulated water level is computed as a function of the water volume exchanged with the main river  
435 and/or adjacent storage areas. Volume-level curves were estimated referring to LiDAR imagery (2 m  
436 resolution) for the dyke-protected floodplains and to a 10 m resolution DEM (Tarquini et al., 2007) for  
437 C-Buffer compartments. The quasi-2D model was calibrated referring to the historical flood event

438 occurred in October 2000 and then used for simulating a major flood event, hereafter referred to as  
439 Tr500, which represents a low frequency/high intensity event associated to a return period of ~500  
440 years (see Castellarin et al., 2011b for details).

441 The main embankment system of the middle and lower portion of the Po River is designed to  
442 cope with flood events associated with return periods up to ~200 years, which are significantly less  
443 intense than the Tr500 event identified in Castellarin et al. (2011a and 2011b). Considering the  
444 homogenous protection level ensured by the major embankment system along the entire study reach  
445 we referred to the Tr500 event as the reference flood scenario, thus limiting the estimation of the  
446 residual flood risk to the likelihood of this extreme event, neglecting the hazard related to flood events  
447 associated to return period lower than 500-year but not contained by the embankment system or to  
448 possible levee failures. Considering these latter possibilities (e.g. breaches on the embankment due to  
449 seepage, piping, etc.) in our study we do not explicitly consider the possibility of levee failures for  
450 more frequent events. Nevertheless, the proposed approach is perfectly suitable for applications that  
451 for example adopt comprehensive multivariate Monte Carlo resampling techniques for a thorough  
452 characterization of the flooding hazard in the region of interest (see e.g. Vorugushyn et al., 2010;  
453 Domeneghetti et al., 2013).

454 The Tr500 inundation scenario is modelled by simulating failures along the embankment system  
455 (i.e. formation of breaches in case of overtopping of main embankments, see configuration BREACHBL  
456 in Castellarin et al., 2011b). Dike overtopping may occur in BREACHBL if the water level exceeds the  
457 crest elevation of the embankments, under this circumstance, as consequence of the flow erosion on  
458 the out-board side of the levee, the quasi-2D model simulates the formation of a levee-breach  
459 according to literature information on width, depth and time of full development recorded for the Po  
460 river (see e.g. Govi and Turitto, 2000). The numerical model enables the simulation of multiple  
461 breaching events as a result of concurrent overtopping phenomena along the main embankment  
462 system, thus enabling the inundation of several C-Buffer compartments during a single major flood  
463 event (see details in Castellarin et al., 2011b). In order to better highlight the role of the exposure to  
464 floods on the evolution of the flood risk the numerical simulations are performed, for both the periods

465 of interest (i.e. 1954 and 2008), referring to the actual levee system configuration, thus neglecting the  
466 strengthening of the levee system eventually performed during last 50 years. Furthermore, the  
467 absence of consistent and statistically significant long-term trends on the streamflow series recorded  
468 along the Po river (see also Section 3.2) enables the use of the same inundation scenario for the entire  
469 period of interest (i.e. from 1954 to 2008), thus facilitating the evaluation of the flood exposure  
470 evolution on the overall flood risk.

471

## 472 **5.2 Estimation of direct economic losses**

473 It is well known that the estimation of direct damages associated with a flood event is a  
474 challenging task which is affected by a large amount of uncertainty (Cammerer et al., 2013).  
475 Concerning Italy, Molinari et al. (2014) related this uncertainty with the lack of high quality post-flood  
476 event damage data, which are necessary for a proper calibration and validation of damage models. In  
477 our analysis, considering the scale of interest (i.e. large scale analysis: middle-lower portion of the Po  
478 river) and the nature of the proposed approach (i.e. simplified numerical tools to evaluate the flood  
479 risk), the quantification of the flood exposure is performed by referring exclusively to the economic  
480 value of private buildings prone to inundation events, neglecting other direct (e.g. damages to public  
481 or commercial buildings) and indirect costs.

482 The Italian Revenue Agency (*Agenzia delle Entrate*, AE) publishes the economic value ( $E$  [€/m<sup>2</sup>])  
483 of different types of private buildings (e.g. civil houses, offices, stores, etc.) in each Italian  
484 administrative district (spatial scale of municipality) every six months (economic values of public  
485 buildings are not provided by AE and thus excluded from the present investigation). Table 4 reports an  
486 example of monetary estimates available for buildings of each municipality conditioned upon the  
487 definition of use (i.e. residential, commercial, services or productive) and typology (i.e. detached  
488 house, box, stores, etc.). Focusing on residential buildings and assuming an unique building type (i.e.  
489 civil houses on Table 4), we define the reference economic value ( $E$  [€/m<sup>2</sup>]) for urban settlements  
490 within any given compartment of the C-Buffer as the average of the  $E$  values provided for all the

491 municipalities, weighted proportionally to their urban extent located within the C-Buffer (see Table 5).  
492 Therefore, the overall value of urban properties can then be approximated by the product of the  
493 average economic value and the overall urban area extent in the compartment, which we obtained  
494 from the land-use maps available for 1954 and 2008 (see Section 4.1).

495 It is worth noting that the damage evaluation relies on the assumption of a constant economic  
496 value for urban buildings over the period of interest (i.e. 1954 and 2008). Without lack of generality,  
497 our analysis considers two different land use maps, yet, for the sake of comparison, we refer to 2014  
498 economic value of buildings for both historical land-use scenarios.

499 The literature provides a wide set of depth-damage curves that offers the possibility to cover  
500 differ applications contexts, considering different types of buildings (i.e. residential, commercial,  
501 industrial, etc.; see e.g. Thielen et al., 2008) and the effect of factors which may influence the expected  
502 damages (i.e. contamination, levels of private precaution, etc.; see e.g. Kreibich et al., 2010). These  
503 curves generally express the percentage of damage of a specific asset as a function of the water depth  
504 and are constructed on empirical damage data (i.e. historical inundation) or using expert judgment  
505 and synthetic analysis.

506 Among the available curves, we refer to the damage-curve implemented in the Multi-Colored  
507 Manual (MCM; Penning-Roswell et al., 2010) that estimates the expected losses for residential  
508 buildings as a function of the local water depth (see Figure 4). The MCM is one of the most advanced  
509 models for flood-damage estimation within Europe (Jongman et al., 2012) and represents a viable tool  
510 for the estimation of the losses related to floods.

511

512

*Figure 4*

513

514 Combining the MCM susceptibility curve and the overall economic value of residential buildings,  
515 we compute the expected damage in a given C-Buffer compartment for a given inundation scenario  
516 through a procedure that is schematically illustrated in Figure 5. The horizontal blue line of Figure 5a

517 represents the maximum water level [m a.s.l.] resulting from the quasi-2D simulation of the  
 518 inundation scenario of interest (see also Section 5.1). As already pointed out, the extent of the  
 519 inundated urban area ( $A_{tot}$ ) can be easily retrieved from the intersection between the elevation of the  
 520 maximum water level (blue line in Figure 5a) and the HVC of the flooded compartment. The damage  
 521 ( $D$ ) to urban settlements is associated with the local water depth ( $h$ ) by means of the depth-damage  
 522 curve (see Figure 5b for a schematic example). This curve also identifies a water-depth value ( $h_{100}$ )  
 523 associated with 100% of damage, meaning that for buildings hit by water depths equal or higher than  
 524  $h_{100}$  the flood-loss coincides with the value of the buildings. Based on this hypothesis, one can estimate  
 525 the extent of urban area where the damage is maximum ( $A_{100}$  [km<sup>2</sup>] in Figure 5a) by subtracting  $h_{100}$   
 526 (i.e. water depth equal to 3 m for the MCM depth-damage curve; see Figure 4) to the maximum flood  
 527 elevation (blue line in Figure 5a). Everywhere in  $A_{100}$  the water depth is higher than  $h_{100}$  and therefore  
 528 the flood damage can be estimated as:

$$D_{100} = E \cdot A_{100} \quad (1)$$

529 where  $E$  [€/m<sup>2</sup>] indicates the overall average economic value of residential buildings in the  
 530 compartment (see Table 4). In the remaining portion of the inundated urban area ( $A_{tot} - A_{100}$  in Figure  
 531 5a) the flood damage,  $D_h$ , depends on the local water depth and can be expressed as:

$$D_h = \int_{A_{100}}^{A_{tot}} E \cdot d[h(A)] dA \quad (2)$$

532 where the percentage of losses  $d(\cdot)$  is a function of  $h(A)$  through the depth-damage curve (see Figure  
 533 4). According to eq. (1) and (2) we calculate the total direct damage in the compartment,  $D$ , as:

$$D = D_{100} + D_h \quad (3)$$

534 It is worth noting that the damage estimate provided by eq. (3) could be easily extended to other  
 535 buildings typologies (see Table 4) or land-uses by considering a better knowledge of these assets

536 within a given compartment and their economic values, that is resorting to a set of different  
537 hypsometric and depth-damage curves, possibly differentiated within the same compartment.

538 *Table 4, Table 5, Figure 5*

539

## 540 **6 Results of the flood-exposure analysis**

### 541 **6.1 Urban areas dynamics**

542 Table 6 summarizes the main features of the Tr500 inundation scenario, listing the C-Buffer  
543 compartments that are flooded due to overtopping of the levee crests and consequent levee breaching  
544 (see Section 5.1 and Castellarin et al., 2011b for details). For each flooded compartment, Table 6  
545 reports the maximum water depth, the total overflow volume and the maximum water inundation  
546 level simulated by the quasi-2D model (see also Figure 5a for a schematic representation of these  
547 terms). Table 6 also reports an estimate of the overall extent of urban areas flooded in 1954 and 2008  
548 under the inundation scenario Tr500, which are obtained by combining the maximum water  
549 inundation levels computed in Castellarin et al. (2011b) with the Hypsometric Vulnerability Curves  
550 (HVCs) proposed in this study ( $A_{\text{tot}}$  in Figure 5).

551 *Table 6*

552 Inundation occurs in 8 compartments as a consequence of just as many levee breaches; estimates  
553 of the overall urban extent affected by the inundation scenario are equal to 1064 ha in 2008 and 496  
554 ha in 1954.

555 According to eq. (1-3) and the MCM depth-damage curve (see Figure 4 and Figure 5), Figure 6  
556 illustrates the overall losses,  $D$  [Billions of Euro], estimated for the flooded compartments by referring  
557 to the average economic value of urban buildings  $E$  (€/m<sup>2</sup>) reported in Table 5. In particular,  
558 considering the urban extent mapped for 1954 and the related HVCs, the overall damage associated  
559 with urban buildings is equal to ~3.6 B€ (present value), with around 65% of the total losses  
560 concentrated in the compartments number 8 and 20 (see Figures 1 and 6). As a consequence of the



561 urban expansion, the losses estimated for the 2008 urban extent rise to ~8.1 B€ (present value), more  
562 than twice the 1954 losses. Compartments 8 and 20 are responsible for ~74% of the total damage in  
563 2008. The higher damage in these compartments can be justified by considering the high economic  
564 value of urban settlements (compartments 20 and 8 have the highest and the fourth-highest E values  
565 among those provided by AE for the residential buildings, respectively; see Table 5) and the amount of  
566 urbanized areas exposed to flood. In fact, looking at Table 6, the flooded urban areas of these  
567 compartments are larger than the others for both reference years (1954 and 2008), thus resulting in  
568 high damages. Furthermore, the striking flood-risk evolution observed in these compartments in the  
569 period 1954-2008 (see Figure 6) can also be explained by considering the spatial evolution of the  
570 urban areas, that is the location where this urban extension predominately occurred. As an example,  
571 Figure 7 reports the HVCs for urban areas of compartments 8 and 10 in the period 1954 and 2008,  
572 while the blue dashed lines in both panels represent the maximum inundation levels obtained from  
573 the quasi-2D model (see also Figure 5a). The comparison of those HVCs highlights that the urban  
574 expansion on the compartments 8 mainly occurred in the most depressed portion of the compartment,  
575 thus exacerbating the flood exposure of urban settlements (a similar land-use evolution characterized  
576 the compartment 20). On the contrary, referring to compartment 10, the urban development occurred  
577 in the highest portion of the compartment (i.e. mainly above 45 m a.s.l.; see Figure 7) with the  
578 consequence that the flood exposure did not increase significantly during the reference period.

579 The analysis of these different dynamics clearly emphasizes the importance of a correct land-use  
580 planning for flood-risk mitigation and highlights the suitability of HVCs as a tool for the identification  
581 of alternative flood-risk attenuation strategies (see Section 7 for a more comprehensive discussion).

582

583

*Table 6 - Figure 6, Figure 7*

584

## 585 6.2 Population dynamics

586 Panel a) of Figure 8 illustrates the temporal dynamics of the number of inhabitants of Emilia-  
587 Romagna and Lombardy administrative districts (grey line), where the C-Buffer is located (see Figure  
588 1), showing a nearly constant grow rate from 1861 to 2011. Focusing on the C-Buffer, the black line on  
589 Figure 8a highlights a different evolution, with a negative population trend that started during '50s  
590 and lasted since 2001. A similar pattern can be seen looking at the panel b) of Figure 8, which  
591 compares the population density in the C-Buffer and in Emilia-Romagna and Lombardy.

592 Figure 9 reports the estimated number of people living in the C-Buffer that are potentially affected  
593 by the Tr500 inundation scenario. These values are estimated by combining the maximum water level  
594 simulated for one of the 8 flooded compartments with its corresponding HIC (Hypsometric Inhabitants  
595 Curve; see Section 4.2). Black and grey bars in Figure 9 represent the simulated number of people  
596 affected by the inundation scenario in 1954 and 2008, respectively. As showed in the figure, the  
597 number of inhabitants exposed to flood in 2008 (grey bars) is lower than the one estimated for 1954  
598 for all compartments but no. 20, where the increase in the number of inhabitants is mainly due to the  
599 presence of Parma, which is a rather large city. The cumulated number of potentially affected people  
600 that can be computed moving downstream along the study reach (i.e. going from Compartment 1 to  
601 20) is illustrated as a black line for 1954 and grey line for 2008, totalizing ~30 400 people in 1954 and  
602 ~ 29 400 people in 2008.

603 *Figure 8, 9*

## 605 7 Flood-risk evolution during the last half-century: Discussion

### 606 7.1 Flood-hazard vs. flood-exposure dynamics

607 Consistently with previous investigations performed for the Po river (see e.g. Montanari et al.,  
608 2012; Zanchettini et al., 2008), the results of trend detection analyses performed along the study reach  
609 point out the absence of statistically significant temporal trends, aside from a slight increase of the

610 annual variability of daily streamflows recorded at the Pontelagoscuro. Therefore the flood-hazard  
611 evolution along the middle and lower portion of Po river in the last five decades does not seem to play  
612 any significant control on the flood-risk dynamics over the same time span. This supports our  
613 assessment of residual flood-risk changes on the basis of a 500-year inundation scenario identified  
614 referring to streamflow data collected since 1917-21 along the study reach (see Castellarin et al.,  
615 2011a), which we consider for representing the residual flood-hazard for the study area (i.e. the C-  
616 Buffer, or dyke-protected flood prone area along the middle lower portion of the Po river).

617 We show that coupling HVCs with inundation scenarios simulated by means of a simplified  
618 hydraulic model (e.g. quasi-2D) may represent a suitable and effective tool for an approximated  
619 quantitative assessment of direct damages to residential settlements over large geographical areas. In  
620 particular, concerning our case study we show that flood risk associated with direct economic losses to  
621 private buildings doubled since 1954, mainly due to the expansion of urbanized areas in the dyke-  
622 protected floodplain (i.e. C-Buffer). Figure 6 shows a significant variation of economic losses  
623 associated with compartments 8 and 20 (see also Figure 1 and Figure 7), which are the most  
624 urbanized compartments and are characterized by large towns. Generalized expansion of urban areas  
625 notwithstanding, the number of exposed inhabitants decreased in all C-Buffer compartments but 8 and  
626 20, where it remained the same (compartment 8) or increased (compartment 20) during the study  
627 period (see Figure 9). This result might be a consequence of inaccuracies of land-use maps adopted in  
628 this analysis, but it also might be representative of an inefficient land planning and utilization (see e.g.  
629 Bhatta et al., 2010). The consequences of this phenomenon, usually known as “urban sprawl”, can be  
630 seen through changes in land-use and land-cover of a specific region, increasing the built-up and paved  
631 area (Sudhira and Ramachandra, 2007), without a corresponding increase of inhabitants (see also  
632 Figure 8). In fact, the birth and growth of residential settlements in rural areas is a common  
633 phenomenon in Northern Italy, even though expansion of metropolitan areas is definitely more  
634 evident (ISTAT, 2008; Settis, 2012). ISTAT (2008) found that the urban areas mapped during the 2001  
635 census covered nearly the 6.4% of the Italian territory with an increase of about 15% compared to  
636 1991, whereas, in the same period, the population grew only 0.4%. Differently from metropolitans

637 area characterized by high population density, rural areas in the North-Eastern part of the country (i.e.  
638 Lombardy, Veneto and Romagna) experienced an unbridled soils consumption due to a low density  
639 urban development (urban sprawl; ISTAT, 2008). These new settlements represent, in some cases, the  
640 outcomes of inefficient and speculative urban, and even industrial in some cases, expansion plans,  
641 which did not result in economic (i.e. well-being) and social developments (see Settis, 2012). As a  
642 consequence, the extent of residential areas reported in land-use maps are not always representative  
643 of a higher number of inhabitants.

644

## 645 **7.2 Main assumptions and limitation of the proposed simplified approach for flood-** 646 **damages computation**

647 Despite the potential of the methodology, there are some limitations that have to be considered  
648 given the assumptions adopted in our study. First, the spatial distribution of different building types  
649 (e.g. commercial, stores, offices, etc.) over the area of interest cannot be inferred from land use maps  
650 that are typically adopted for large scale analysis (e.g. Corine Land Cover). The lack of accurate  
651 information concerning the location of specific building categories constrains the possibility to  
652 evaluate their exposure to floods through specific HVCs (i.e. different HVCs defined for civil or  
653 detached houses, garages or other buildings category such as those reported in Table 4).

654 Second, the adoption of AE estimates (see Table 5) inevitably undervalues the overall losses for  
655 urban areas, and in particular for residential buildings, since a series of other direct (e.g. chattel,  
656 furniture, stocks, etc.) and indirect (e.g. economic losses indirectly related to the loss of private  
657 houses) costs are not considered and economically quantified. The estimate provided by AE  
658 represents the present real estate market value of a given building type, that is more an expression of  
659 the overall economic well-being of a specific area rather than the actual economic loss in case of a  
660 flood event. This bias is expected to be more significant for the productive infrastructures (i.e.  
661 industries), where a number of different variables (such as for example the type of production, the

662 technology level of the industries, the amount of stocks, the day of work interruption, etc.) strongly  
663 influence the overall damages associated to inundation events.

664 Finally, using an averaged economic value for all urban assets within a given compartment may  
665 introduce biases in the economic assessment of the flood impacts. The expansion and development of  
666 urban areas at higher elevations in the compartment (and thus in “safer” locations) may increase the  
667 overall economic value use of urban settlements within the compartment. Consequently, averaging the  
668 economic value over all residential areas in the compartment would increase the economic value also  
669 of rural residential areas situated in the lowland portion of the compartment, with the paradox that a  
670 correct land-use development policy may increase the risk in the flood-prone areas. This limitation can  
671 be easily overcome by constructing different HVCs for different municipalities (or economically  
672 different residential areas) within each compartment and by using them in parallel. Furthermore,  
673 when using a single HVC for all urban settlements within a given compartment, as in this study, bias  
674 can be effectively reduced by referring to a single economic value, as we did (i.e. 2014), for all  
675 considered historical land-use scenarios (i.e. 1954 and 2008 in this study). Under this hypothesis, the  
676 analysis of the urban development over the period of interest is considered exclusively in terms of  
677 elevation, that is considering in which part of the compartment the urban area expanded (i.e. in areas  
678 that are more or less prone-to-floods), without considering its economic development during the last  
679 half century.

680 Despite these limitations, the proposed methodology appears appropriate for the purpose of the  
681 analysis, that is not aimed at providing a comprehensive and exhaustive quantification of the flood risk  
682 or of the overall flood losses expected in case of an extreme flood event, but rather to propose a tool  
683 which enables the inferring of factors that mainly driven the evolution of the residual flood risk in a  
684 specific area, or for investigating alternative flood-risk mitigation strategies at basin scale (see Section  
685 7 for more details).

686

### 687 7.3 The “levee paradox” along the Po river

688 Following the concept of the “levee effect” (see e.g., Tobin, 1995), the feeling of safety ensured by  
689 levee systems may encourage the economic and social growth on the floodplain areas, leading to the  
690 potential condition for a faster development of human settlements. However, considering our study  
691 area, we already stated that while during the last fifty years we observe an increase of the total  
692 economic losses associated with a given inundation scenario (see Figure 6), the “levee effect”  
693 paradigm is not supported by the associate population dynamics. Considering Figure 8, the population  
694 growth on the area closer to the river appears comparable with the one measured in the remaining  
695 part of the basin (i.e. Emilia-Romagna and Lombardy) until 1950. Starting from the 50’s, people moved  
696 from the floodplains toward the major cities and settled far away from the main river, causing a  
697 significant decrease of number of people exposed to floods. The “shock” induced by the flood disaster  
698 occurred in the 1951 to the floodplain socioeconomic system (see e.g., Amadio et al., 2013; Di  
699 Baldassarre et al., 2013) is clearly visible in Figure 8. Together with an increased flood-risk awareness  
700 resulted from the 1951 inundation event, the rapid industrial and economic growth that characterized  
701 the aftermath of the II World War is undoubtedly another important driver that attracted people from  
702 rural areas towards richer and more industrialized areas, such as large cities.

703 Figure 10 further investigates the levee paradox in the study area. Panel a), in particular,  
704 compares the growth rate of the urban settlements in the C-Buffer with the one observed in the Emilia-  
705 Romagna and Lombardy districts during the last half-century. Urban extent in the C-Buffer doubled in  
706 the last fifty years (increase of about 180%), while the growth rate observed in Emilia-Romagna and  
707 Lombardy districts is higher than or equal to 230%. Even though the urban development in the flood-  
708 prone area is evident and representative of a levee-effect, it appears to be less pronounced than in  
709 other parts of the basin. These findings seem to support the idea that the expansion of residential  
710 areas is related mainly to social and economic drivers, than to the proximity to the water, that no  
711 longer represents a peculiarity of favorable development conditions in developed society (Di  
712 Baldassarre et al., 2013). A different behavior could otherwise be expected considering the industrial  
713 sector, where the availability of a large amount of fresh water still represents a key element for

714 developing productive activities. Panel b) of Figure 10 confirms these considerations for the study  
715 area. Referring to the results of a preliminary investigation, panel b) of Figure 10 compares the extent  
716 and growth rate of industries in the C-Buffer and in the Emilia-Romagna and Lombardy districts,  
717 showing an opposite trend relative to what can be observed for residential areas. Even though  
718 industrial areas grew over 712% in Emilia-Romagna and Lombardy, the industrial activities  
719 experienced a higher grow-rate (1350%) in the areas closer to the river (i.e. C-Buffer). The presence of  
720 a levee system, together with the proximity to abundance of fresh water, is evidently an incentive to  
721 the development of industries, which is also encouraged by the lower costs of formerly rural areas.  
722 The dynamic of the industrial asset strongly impacts the evolution of the residual flood risk and will be  
723 the objective of specific future analyses.

724

*Figure 9*

## 725 **8 Conclusions**

726 Our study considers the middle-lower portion of the Po river and analyzes the evolution of the  
727 residual flood-risk during the last half century for residential areas in the Pianura Padana, a large and  
728 socio-economically very important dyke-protected flood-prone area located in Northern Italy, by  
729 investigating changes in flood frequency (i.e. flood hazard) and exposure to floods.

730 Consistently with previous analyses (see e.g. Montanari, 2013; Zanchettini et al., 2008) our trend  
731 detection analysis, which we carried out on long historical series observed for the Po river, does not  
732 detect any evidence of a statistically significant change in the flood hazard along the Po river and  
733 supports the stationarity of the hydrological series during the period of interest (i.e. last five decades).

734 Changes in the residual flood risk, if any, could be mainly ascribed to an evolution of the exposure  
735 to floods. Therefore, we analyzed the possible alteration of exposure to floods in the study area,  
736 looking in particular at number of inhabitants and extension of residential areas. We propose the use  
737 of simplified graphical tools (i.e. Hypsometric Vulnerability Curves-HVCs and Hypsometric Inhabitants  
738 Curve-HICs) for a quantitative, yet approximate, large-scale assessment of the direct tangible

739 economic losses to private residential buildings and of the number of people affected by a given  
740 inundation scenario. HVCs and HICs can be constructed using a minimal set of information (i.e. a  
741 digital elevation model, land-use map, census data) for any given flood-prone compartment  
742 represented in a quasi two-dimensional numerical schematization as a storage area. Despite the  
743 usefulness and ease of the proposed methodology it is worth noting that its application in our study  
744 relies on a number of simplifying assumptions that need to be acknowledged in order not to  
745 misinterpret the results (see also Section 5.2):

746 a) the flood-hazard assessment is performed by means of a simplified quasi-2D model (see  
747 Castellarin et al., 2001b) in which the flood-prone compartments are reproduced as storage areas  
748 regulated by means of volume-water level defined on a DEM with a resolution of 10 m (see  
749 Section 5.1);

750 b) aggregation classes adopted by land-use maps (see Table 3) do not enable the identification of  
751 specific building typology, such as for example detached house, garages, office, stores, etc. (see  
752 Table 4); as a result, the economic estimates consider a single (average) building typology for  
753 each compartment.

754 c) the economic estimates provided by AE represent the market value of the urban buildings in a  
755 given municipality and are not representative of the actual potential damages expected in case of  
756 inundations (e.g. damages to furniture are not considered);

757 d) the population density adopted for the HICs is assumed to be uniform within a given  
758 municipality neglecting differences between rural and central urban areas.

759 These limitations notwithstanding, our preliminary application demonstrates the usefulness of  
760 HVCs and HICs and their potential for flood-vulnerability and flood-risk assessment. The accuracy of  
761 the proposed methodology can be easily increased by referring to more accurate data (e.g. finer land-  
762 use discretization, advanced economic estimate; etc.), different HVCs defined for each municipality or  
763 land use type, or to detailed simulation of the inundation characteristics (e.g. flood dynamics simulated  
764 by means of 2D hydraulic models).



765 The analysis points out a significant growth of the extension of residential areas over the study  
766 region, with a consequent increase in the expected damage that is almost doubled relative to the  
767 considered inundation scenario (recurrence interval ~500 years). On the contrary, the number of  
768 exposed inhabitants showed only marginal modifications during the study period. These findings offer  
769 important elements to further the discussion on the existence and importance of the “levee effect” (or  
770 call-effect, Tobin, 1995) along the middle-lower portion of the Po river. The study outcome also foster  
771 some general considerations on the arguable applicability of the call-effect for developed and  
772 technologically advanced countries, where the physical proximity to fresh water may not represent  
773 the predominant factor for the development of residential settlements (Di Baldassarre et al., 2013).  
774 Despite our study focused on the development of urban settlements only, different evidences seem to  
775 arise from preliminary analysis performed relative to the industrial asset, from which we have noticed  
776 in the C-Buffer a greater growth rate than the one occurred in the rest of Emilia-Romagna and  
777 Lombardy districts. However, further investigations are needed addressing this specific point for  
778 getting a more definite answer concerning the existence and entity of a call-effect relative to industrial  
779 activities in the study area during the last fifty years. Further analyses are also required to enable the  
780 assessment of flood-losses that are potentially expected in commercial and industrial areas, for which  
781 the economic values provided by the Italian Revenue Agency (AE) appear far from being useful as  
782 indicators of the expected losses (see also Section 5.2).

783 Over the past two decades the flood-risk management experienced a shift from a hazard-driven  
784 view to a risk-based perspective, in which the risk management policies are increasingly identified and  
785 evaluated in the light of system susceptibility and resilience, thus focusing on the capacity of the  
786 system to coexist with, and recover from, inundations (see e.g. Merz et al., 2010). The European Flood  
787 Directive 2007/60 further promotes this process requiring the Member States to identify flood-risk  
788 mitigation plans in order to reduce the adverse consequences (e.g. number of people affected,  
789 damages, etc.) of a given inundation event. In this context, keeping in mind all the assumptions that  
790 were previously highlighted, the combination of HVCs (and HICs) with inundation scenarios computed  
791 through simplified hydraulic models can be a viable strategy for quantitative large-scale assessments

792 of the residual flood risk. The proposed methodology may be useful for decision-makers in charge of  
793 the definition of large scale flood-risk mitigation strategies, as the resort to HVCs can provide  
794 stakeholders with a preliminary estimation of the impact of a given inundation event and enables  
795 them to easily compare the effectiveness of alternative flood risk mitigation strategies (e.g. controlled  
796 flooding vs. strengthening of the existing levee system, see e.g. Vis et al., 2003; Merz et al., 2010;  
797 Castellarin et al., 2011a).

798

799

800 **Acknowledgements:** The study was carried out as part of the activities of the working group  
801 Anthropogenic and climatic controls on water availability (ACCuRACy) of scientific decade 2013–2022  
802 of IAHS, entitled “Panta Rhei – Everything Flows” - Change in Hydrology and Society (see Montanari et  
803 al., 2013). The authors are extremely grateful to the Interregional Agency for the Po River (Agenzia  
804 Interregionale per il Fiume Po, AIPO, Italy) and Po River Basin Authority (Autorità di Bacino del Fiume  
805 Po, Italy) allowing access to their high resolution DTM of River Po and GIS layers used in the analysis.  
806 Finally, the Authors acknowledge the appropriateness and the usefulness of anonymous Reviewers'  
807 comments.

- 809 AdB-Po, 1999. Progetto di Piano stralcio per l'Assetto Idro-geologico (PAI) – Interventi sulla rete  
810 idrografica e sui versanti, AdB-Po, Parma, Italy (in Italian).
- 811 AdB-Po, 2006. Behaviours of the Po River catchment and first investigation of the impact of human  
812 activities on water resources, Adb-Po, Parma, Italy (in Italian).
- 813 Amadio, M, Mysiak, J., Pecora, S., Agnetti, A., 2013. Looking Forward from the Past: Assessing the  
814 Potential Flood Hazard and Damage in Polesine Region by Revisiting the 1950 Flood Event.  
815 Fondazione Eni Enrico Mattei Working Papers. Paper 852.  
816 <http://services.bepress.com/feem/paper852>.
- 817 Apel, H., Merz, B., Thielen, A. H., 2008. Quantification of uncertainties in flood risk assessments, *Int. J.*  
818 *River Basin Management*, 6, 149–162.
- 819 Barredo, J. I., 2009. Normalised flood losses in Europe: 1970–2006. *Nat. Hazards Earth Syst. Sci.*, 9(1),  
820 97–104. doi:10.5194/nhess-9-97-2009
- 821 Bhatta, B., Saraswati, S., Bandyopadhyay, D., 2010. Urban sprawl measurement from remote sensing  
822 data, *Appl. Geogr.*, 30(4), 731–740, doi:10.1016/j.apgeog.2010.02.002.
- 823 Bouwer, L. M., Bubeck, P., Aerts, J. C. J. H., 2010. Changes in future flood risk due to climate and  
824 development in a Dutch polder area. *Global Environ. Change*, 20(3), 463–471.  
825 doi:10.1016/j.gloenvcha.2010.04.002
- 826 Cammerer, H., Thielen, A. H., Lammel, J., 2013. Adaptability and transferability of flood loss functions  
827 in residential areas. *Natural Hazards and Earth System Sciences*, 13, 3063–3081.  
828 doi:10.5194/nhess-13-3063-2013
- 829 Carrera, L., Standardi, G., Bosello, F., & Mysiak, J., 2013. Assessing direct and indirect economic impacts  
830 of a flood event through the integration of spatial and computable general equilibrium modelling.  
831 *Environmental Modelling & Software*, 63(2015), 109–122. doi:10.1016/j.envsoft.2014.09.016
- 832 Castellarin, A, Di Baldassarre, G., Brath, A., 2011a. Floodplain management strategies for flood  
833 attenuation in the river Po. *River Res. Appl.*, 27(8), 1037–1047. doi:10.1002/rra.1405.
- 834 Castellarin, Attilio, Domeneghetti, A., Brath, A., 2011b. Identifying robust large-scale flood risk  
835 mitigation strategies: A quasi-2D hydraulic model as a tool for the Po river. *Physics Phys. Chem.*  
836 *Earth, Parts A/B/C*, 36(7-8), 299–308. doi:10.1016/j.pce.2011.02.008.
- 837 Coratza, L., 2005. Aggiornamento del catasto delle arginature maestre di Po, Parma (in Italian).
- 838 De Moel, H., Aerts, J. C. J. H., & Koomen, E., 2011a. Development of flood exposure in the Netherlands  
839 during the 20th and 21st century. *Global Environ. Change*, 21(2), 620–627.  
840 doi:10.1016/j.gloenvcha.2010.12.005
- 841 De Moel, H., Aerts, J. C. J. H., 2011b. Effect of uncertainty in land use, damage models and inundation  
842 depth on flood damage estimates, *Nat. Hazards*, 58, 407–425, doi:10.1007/s11069-010- 9675-6.
- 843 De Moel, H., Asselman, N. E. M., Aerts, J. C. J. H., 2012. Uncertainty and sensitivity analysis of coastal  
844 flood damage estimates in the west of the Netherlands. *Nat. Hazards Earth Syst. Sci.*, 12(4), 1045–  
845 1058. doi:10.5194/nhess-12-1045-2012

- 846 Di Baldassarre, G., Castellarin, A., Montanari, A., Brath, A., 2009. Probability weighted hazard maps for  
847 comparing different flood risk management strategies: a case study. *Nat. Hazards*.  
848 doi:10.1007/s11069-009-9355-6.
- 849 Di Baldassarre, G., Castellarin, A., Brath, A., 2010. Analysis of the effects of levee heightening on flood  
850 propagation: example of the River Po, Italy, *Hydrol. Sci. J.*, 54(6).
- 851 Di Baldassarre, G., Kooy, M., Kemerink, J. S., Brandimarte, L., 2013. Towards understanding the  
852 dynamic behaviour of floodplains as human-water systems. *Hydrol. Earth Syst. Sci.*, 17(8), 3235–  
853 3244. doi:10.5194/hess-17-3235-2013
- 854 Domeneghetti, A., Vorogushyn, S., Castellarin, A., Merz, B., Brath, A., 2013. Probabilistic flood hazard  
855 mapping: effects of uncertain boundary conditions, *Hydrol. Earth Syst. Sci.*, 17(8), 3127–3140,  
856 doi:10.5194/hess-17-3127-2013.
- 857 Douglas, E. M., Vogel, R. M., Kroll, C. N., 2000. Trends in floods and low flows in the United States:  
858 impact of spatial correlation, *J. Hydrol.*, 240, 90–105.
- 859 European Environment Agency (EEA), 2009. CORINE land cover 2006 (CLC2006) 100 m, [112/2009],  
860 Copenhagen, Denmark.
- 861 Elmer, F., Hoymann, J., DÜthmann, D., Vorogushyn, S., Kreibich, H., 2012. Drivers of flood risk change in  
862 residential areas. *Nat. Hazards Earth Syst. Sci.*, 12(5), 1641–1657. doi:10.5194/nhess-12-1641-  
863 2012
- 864 Elmer, F., Thielen, A. H., Pech, I., Kreibich, H., 2010. Influence of flood frequency on residential building  
865 losses. *Nat. Hazards Earth Syst. Sci.*, 10, 2145–2159, 2010.
- 866 EEA- European Environment Agency, 2005. Vulnerability and Adaptation to Climate Change: Scoping  
867 Report. EEA Tech. Report, Copenhagen, Denmark.
- 868 European Exchange Circle on Flood Mapping (EXCIMAP), 2007. Handbook on Good Practices for Flood  
869 Mapping in Europe, EXCIMAP, available at: <http://caphaz-net.org/outcomes-results>.
- 870 European Parliament, Council, 2007. Directive 2007/60/Ec of the European Parliament and of the  
871 Council of 23 October 2007 on the Assessment and Management of Flood Risks. <[http://eur-  
872 lex.europa.eu/en/index.htm](http://eur-lex.europa.eu/en/index.htm)>.
- 873 Govi, M., Turitto, O., 2000. Casistica storica sui processi d'iterazione delle correnti di piena del Po con  
874 arginature e con elementi morfotopografici del territorio adiacente (Historical documentations  
875 about the processes of dam breaks in the River Po, in Italian), Istituto Lombardo Accademia di  
876 Scienza e Lettere, Milano, Italy.
- 877 Hall, J.W., Sayers, P.B., Dawson, R.J., 2005. National-scale assessment of current and future flood risk in  
878 England and Wales. *Nat. Hazards*. 36, 147-164.
- 879 Hamed, K. H., 2008. Trend detection in hydrologic data: The Mann–Kendall trend test under the scaling  
880 hypothesis. *J. Hydrol.*, 349, 350– 363. doi:10.1016/j.jhydrol.2007.11.009
- 881 Heine, R.A., Pinter, N., 2012. Levee effects upon flood levels: an empirical assessment. *Hydrol.*  
882 *Processes*, 26(21), 3225–3240. doi:10.1002/hyp.8261
- 883 IPCC, 2013: Summary for Policymakers. In: *Climate Change 2013: The Physical Science Basis*.  
884 Contribution of Working Group I to the Fifth Assessment Report of the Intergovernmental Panel  
885 on Climate Change, Stocker, T.F., D. Qin, G.-K. Plattner, M. Tignor, S.K. Allen, J. Boschung, A. Nauels,  
886 Y. Xia, V. Bex and P.M. Midgley (eds.).

- 887 ISTAT, 2008. Rapporto Annuale, la situazione del Paese nel 2008, ISTAT (in Italian).
- 888 Jonkman, S.N., 2005. Global Perspectives on Loss of Human Life Caused by Floods. *Nat. Hazards*, 34(2),  
889 151–175. doi:10.1007/s11069-004-8891-3
- 890 Jongman, B., Kreibich, H., Apel, H., Barredo, J. I., Bates, P. D., Feyen, L., Neal, J., 2012. Comparative flood  
891 damage model assessment: towards a European approach. *Nat. Hazards Earth Syst. Sci.*, 12, 3733–  
892 3752. doi:10.5194/nhess-12-3733-2012
- 893 Kendall, M. G., 1975. *Rank Correlation Methods*, Griffin, London.
- 894 Kundzewicz, Z.W., Graczyk, D., Maurer, T., Pinskiwar, I., Radziejewski, M., Svensson, C., Szwed, M., 2005.  
895 Trend detection in river flow series: 1. Annual maximum flow. *Hydrological Sciences Journal* 50  
896 (5), 797–810.
- 897 Kreibich, H., Seifert, I., Merz, B., Thielen, A. H., 2010. Development of FLEMOcs – A new model for the  
898 estimation of flood losses in companies. *Hydrolog. Sci. J.*, 55, 1302–1314.
- 899 Ludy, J., Kondolf, G. M., 2012. Flood risk perception in lands “protected” by 100-year levees. *Nat.*  
900 *Hazards*, 61(2), 829–842. doi:10.1007/s11069-011-0072-6
- 901 Mann, H. B., 1945. Nonparametric tests against trend, *Econometrica* 13, 245–259.
- 902 Marchi, E., 1991. Hydraulic aspects of the Po River flood occurred in 1951, in: *Proceedings of the XVII*  
903 *Conference on Historical Studies*, Rovigo, 2–24 November 1991, Minnelliana Editions, Rovigo,  
904 1994 (in Italian).
- 905 Markantonis, V., Meyer, V., Schwarze, R., 2012. Valuating the intangible effects of natural hazards -  
906 Review and analysis of the costing methods, *Nat. Hazards Earth Syst. Sci.*, 12, 1633–1640,  
907 doi:10.5194/nhess-12-1633-2012.
- 908 Masoero, A., Claps, P., Asselman, N. E. M., Mosselman, E., Di Baldassarre, G., 2013. Reconstruction and  
909 analysis of the Po River inundation of 1951. *Hydrol. Processes*, 27(9), 1341–1348.  
910 doi:10.1002/hyp.9558
- 911 Merz, B., Elmer, F., Thielen, A. H., 2009. Significance of “high probability/low damage” versus “low  
912 probability/high damage” flood events. *Nat. Hazards Earth Syst. Sci.*, 9(3), 1033–1046.  
913 doi:10.5194/nhess-9-1033-2009
- 914 Merz, B., Hall, J., Disse, M., Schumann, A., 2010. Fluvial flood risk management in a changing world. *Nat.*  
915 *Hazards Earth Syst. Sci.*, 10, 509–527.
- 916 Messner, F., Penning-Rowsell, E. C., Green, C., Meyer, V., Tunstall, S.M., van der Veen, A., 2007.  
917 *Evaluating flood damages: guidance and recommendations on principles and methods*, FLOODsite,  
918 Wallingford, UK, T09-06-01.
- 919 Meyer, V., Becker, N., Markantonis, V., Schwarze, R., Van Den Bergh, J. C. J. M., Bouwer, L. M., ...  
920 Viavattene, C., 2013. Review article: Assessing the costs of natural hazards-state of the art and  
921 knowledge gaps. *Natural Hazards and Earth System Science*, 13, 1351–1373. doi:10.5194/nhess-  
922 13-1351-2013
- 923 Molinari, D., Menoni, S., Aronica, G. T., Ballio, F., Berni, N., Pandolfo, C., Stelluti, M., Minucci, G., 2014. Ex  
924 post damage assessment: an Italian experience. *Natural Hazards and Earth System Science*, 14(c),  
925 901–916. doi:10.5194/nhess-14-901-2014.

- 926 Montanari, A., 2012. Hydrology of the Po River: looking for changing patterns in river discharge,  
927 *Hydrol. Earth Syst. Sci.*, 16, 3739-3747, doi:10.5194/hess-16-3739-2012.
- 928 Montanari, A., Young, G., Savenije, H.H.G., Hughes, D., Wagener, T., Ren, L.L., Koutsoyiannis, D.,  
929 Cudennec, C., Toth, E., Grimaldi, S., Blöschl, G., Sivapalan, M., Beven, K., Gupta, H., Hipsey, M.,  
930 Schaeffli, B., Arheimer, B., Boegh, E., Schymanski, S.J., Di Baldassarre, G., Yu, B., Hubert, P., Huang, Y.,  
931 Schumann, A., Post, D., Srinivasan, V., Harman, C., Thompson, S., Rogger, M., Viglione, A., McMillan,  
932 H., Characklis, G., Pang, Z., and Belyaev, V., 2013. "Panta Rhei—Everything Flows": Change in  
933 hydrology and society—The IAHS Scientific Decade 2013–2022. *Hydrolog Sci J.* 58 (6) 1256–1275.
- 934 Neumayer, E., Barthel, F., 2011. Normalizing economic loss from natural disasters: A global analysis.  
935 *Global Environ. Change*, 21(1), 13–24. doi:10.1016/j.gloenvcha.2010.10.004
- 936 Penning-Rowsell, E., Viavattene, C., Pardoe, J., Chatterton, J., Parker, D., Morris, J., 2010. The benefits of  
937 flood and coastal risk management: a handbook of assessment techniques. Flood Hazard Research  
938 Centre, Middlesex, 2010.
- 939 Petrow, T., Merz, B., 2009. Trends in flood magnitude, frequency and seasonality in Germany in the  
940 period 1951-2002. *J. Hydrol.*, 371, 129-141. doi:10.1016/j.jhydrol.2009.03.024
- 941 Pielke, Jr. R.A., Gratz, J., Landsea, C.W., Collins, D., Saunders, M.A., Musulin, R., 2008. Normalized  
942 hurricane damages in the United States: 1900–2005. *Nat. Hazard. Rev.* 9 (1), 29–42.
- 943 Pielke Jr., R.A., Landsea, C.W., 1998. Normalized hurricane damages in the United States: 1925–1995.  
944 *Weather Forecast.* 621–631.
- 945 Settis S., 2012. *Paesaggio Costituzione cemento. La battaglia per l'ambiente contro il degrado civile*,  
946 Ed.Einaudi, pp. 326, ISBN-13 9788806210373 (in Italian).
- 947 Schultz, J., Elliott, J.R., 2012. Natural disasters and local demographic change in the United States.  
948 *Population and Environment*, 34(3), 293–312. doi:10.1007/s11111-012-0171-7
- 949 Stern, N., 2007. *The Economics of Climate Change – The Stern Review*. Cambridge University Press,  
950 Cambridge.
- 951 Sudhira, H.S., Ramachandra, T.V., 2007. Characterising urban sprawl from remote sensing data and  
952 using landscape metrics, in *Proceedings of the 10th International Conference on Computers in*  
953 *Urban Planning and Urban Management*, p. 12, Iguassu Falls, PR Brazil, July 11-13, 2007.
- 954 Svensson, C., Kundzewicz, Z.W., Maurer, T., 2005. Trend detection in river flow series: 2 Flood and low  
955 – flow index series. *Hydrological Sciences Journal* 50 (5), 811–824.
- 956 Tarquini, S., Isola, I., Favalli, M., Mazzarini, F., Bisson, M., Pareschi, M. T., Boschi, E., 2007. TINITALY /  
957 01: a new Triangular Irregular Network of Italy. *Annal of Geophysics*, 50, 407-425.
- 958 Tarquini, S., Vinci, S., Favalli, M., Doumaz, F., Fornaciai, A., Nannipieri, L., 2012. Release of a 10-m-  
959 resolution DEM for the Italian territory: Comparison with global-coverage DEMs and anaglyph-  
960 mode exploration via the web. *Comput. Geosci.* 38(1), 168–170. doi:10.1016/j.cageo.2011.04.018.
- 961 Thielen, A. H., Olschewski, A., Kreibich, H., Kobsch, S., Merz, B., 2008. Development and evaluation of  
962 FLEMOps – a new Flood Loss Estimation Model for the private sector, edited by: Proverbs, D.,  
963 Brebbia, C. A., and Penning-Rowsell, E., *Flood Recovery, Innovation and Response I*, WIT Press,  
964 315–324.
- 965 Tobin, G.A., 1995. The levee love affair: a stormy relationship. *Water Resour. Bull.* 31, 359–367.

- 966 Villarini, G., Smith, J. A., Serinaldi, F., Ntelekos, A. A., 2011. Analyses of seasonal and annual maximum  
967 daily discharge records for central Europe, *J. Hydrol.*, 399, 299–312,  
968 doi:10.1016/j.jhydrol.2011.01.007.
- 969 Vis, M., Klijn, F., De Bruijn, K. M., Van Buuren, M., 2003. Resilience strategies for flood risk management  
970 in the Netherlands. *Int. J. River Basin Management*, 1(1), 33–40.  
971 doi:10.1080/15715124.2003.9635190.
- 972 Visentini, M., 1953. The latest floods of the Po River, in: *Proceedings of the XVIII International*  
973 *Conference on Navigation, Rome*.
- 974 von Storch, H., Cannon, A.J., 1995. *Analysis of Climate Variability – Applications of Statistical*  
975 *Techniques*. Springer Verlag, New York, 334 pp.
- 976 Vorogushyn, S., Merz, B., Lindenschmidt, K.E., Apel, H., 2010. A new methodology for flood hazard  
977 assessment considering dike breaches, *Water Resour. Res.*, 46(8), 1–17,  
978 doi:10.1029/2009WR008475.
- 979 Vorogushyn, S., Merz, B., 2013. Flood trends along the Rhine: the role of river training. *Hydrol. Earth*  
980 *Syst. Sci.*, 17, 3871–3884, doi:10.5194/hess-17-3871-2013.
- 981 Willems, P., Vaes, G., Popa, D., Timbe, L., Berlamont, J., 2002. Quasi 2D river flood modelling. In:  
982 Bousmar, D., Zech, Y. (Eds.), *River Flow 2002*, vol. 2. Swets and Zeitlinger, Lisse, pp. 1253–1259.
- 983 Wilby, R. L., Beven, K. J., Reynard, N. S., 2008. Climate change and fluvial flood risk in the UK : more of  
984 the same ? *Hydrological Processes*, 22, 2511–2523. doi:10.1002/hyp
- 985 Yue, S., Pilon, P., Phinney, B., Cavadias, G., 2002. The influence of autocorrelation on the ability to detect  
986 trend in hydrological time series. *Hydrol. Processes* 16, 1807–1829.
- 987 Yue, S., Wang, C.Y., 2004. The Mann–Kendall test modified by effective sample size to detect trend in  
988 serially correlated hydrological series. *Water Resour. Manage.* 8 (3), 201–218.
- 989 Zanchettini, D., Traverso, P., Tomasino, M., 2008. Po River discharge: a preliminary analysis of a 200-  
990 year time series, *Climatic Change*, 88, 411–433, doi:10.1007/s10584-008-9395-z
- 991 Zhang, K., Dittmar, J., Ross, M., Bergh, C., 2011. Assessment of sea level rise impacts on human  
992 population and real property in the Florida Keys. *Climatic Change*, 107(2011), 129–146.  
993 doi:10.1007/s10584-011-0080-2

994 **TABLE**

995 **Table 1.** Characteristics of the long daily streamflow series available along the main stretch of the Po river  
996 (observation period, mean ( $\mu$ ), standard deviation ( $\sigma$ ) and range of variation of the daily discharge data series),  
997 along with the catchment area ( $A$ ) at the specific gauging location.

<i>Gauging station</i>	<i>Period</i>	$\mu$ [m <sup>3</sup> /s]	$\sigma$ [m <sup>3</sup> /s]	<i>min-max</i> [m <sup>3</sup> /s]	<i>A</i> [km <sup>2</sup> ]
<i>Moncalieri</i>	1942-1984	80	89	3 - 2 170	4 885
<i>Piacenza</i>	1924-2009	959	773	52 - 12 600	42 030
<i>Pontelagoscuro</i>	1920-2009	1 490	1 007	168 - 9 780	71 000

998

ACCEPTED ARTICLE



999  
1000  
1001

**Table 2.** Results of the Mann-Kendall statistical trend detection tests for AMS, MEAN and SD data series at the gauges section of Moncalieri, Piacenza and Pontelagoscuro (see also Table 1): test significance  $p$ -value, Sen's slope ( $\beta$ ) and variation ( $\Delta$ ) over the period of available data.

	<i>Moncalieri</i>			<i>Piacenza</i>			<i>Pontelagoscuro</i>		
	<i>p-value</i>	$\beta$ [m <sup>3</sup> /s/year]	$\Delta$ [m <sup>3</sup> /s]	<i>p-value</i>	$\beta$ [m <sup>3</sup> /s/year]	$\Delta$ [m <sup>3</sup> /s]	<i>p-value</i>	$\beta$ [m <sup>3</sup> /s/year]	$\Delta$ [m <sup>3</sup> /s]
<b>AMS</b>	0.753	2.09	87.8	0.822	2.02	172.5	0.106	13.2	1178
<b>MEAN</b>	0.397	0.31	13.41	0.770	-0.28	-24.17	0.450	1.27	113
<b>SD</b>	1	-0.02	-0.90	0.796	0.07	5.95	0.043	2.53	225

1002

1003

1004

1005

ACCEPTED ARTICLE

1006  
1007

**Table 3.** Aggregated land-use classes adopted for the characterization of urban settlements in different time periods [x indicates all sub-categories considered by finer land-use classifications].

CORINE (2006)		G.A.I - WWS (1954)		AGEA-2008	
<i>Cod.</i>	<i>Class description</i>	<i>Cod.</i>	<i>Class description.</i>	<i>Cod.</i>	<i>Class description</i>
111	Continuous urban fabric	1a	Continuous and discontinuous urban fabric	111x	Continuous and sparse urban fabric
112	Discontinuous urban fabric	1g	Green urban and sport areas	112x	Discontinuous and isolated residential fabric
14x	Green urban and sport areas			142x	Farmstead, gardens, parks and campground

1008

ACCEPTED ARTICLE

1009  
1010

**Table 4.** Example of economic values ( $E[\text{€/m}^2]$ ) provided by AE in relation to buildings typology in a given municipality (values and buildings typologies may vary from different municipalities).

<b>Category</b>	<b>Building typology</b>	<b>Economic value E [€/m<sup>2</sup>]</b>
Residential	Civil houses	1 975
	Garage, cellar, etc.	850
	Detached houses	2 400
Commercial	Stores	1 750
	Warehouses	925
Tertiary	Offices	1 550
Manufacturing	Productive plant	850

1011  
1012  
1013  
1014  
1015

ACCEPTED ARTICLE

1016  
1017

**Table 5.** Average economic values of civil buildings provided by the Italian Revenue Agency (AE) in the C-Buffer compartments flooded in case of the Tr500 event.

<b>Compartment</b>	<b>Average value <i>E</i> [€/m<sup>2</sup>]</b>
1	~ 840
2	~ 970
3	~ 865
6	~ 870
8	~ 935
10	~ 850
18	~ 1 105
20	~ 1 245

1018  
1019  
1020  
1021

ACCEPTED ARTICLE

1022  
1023

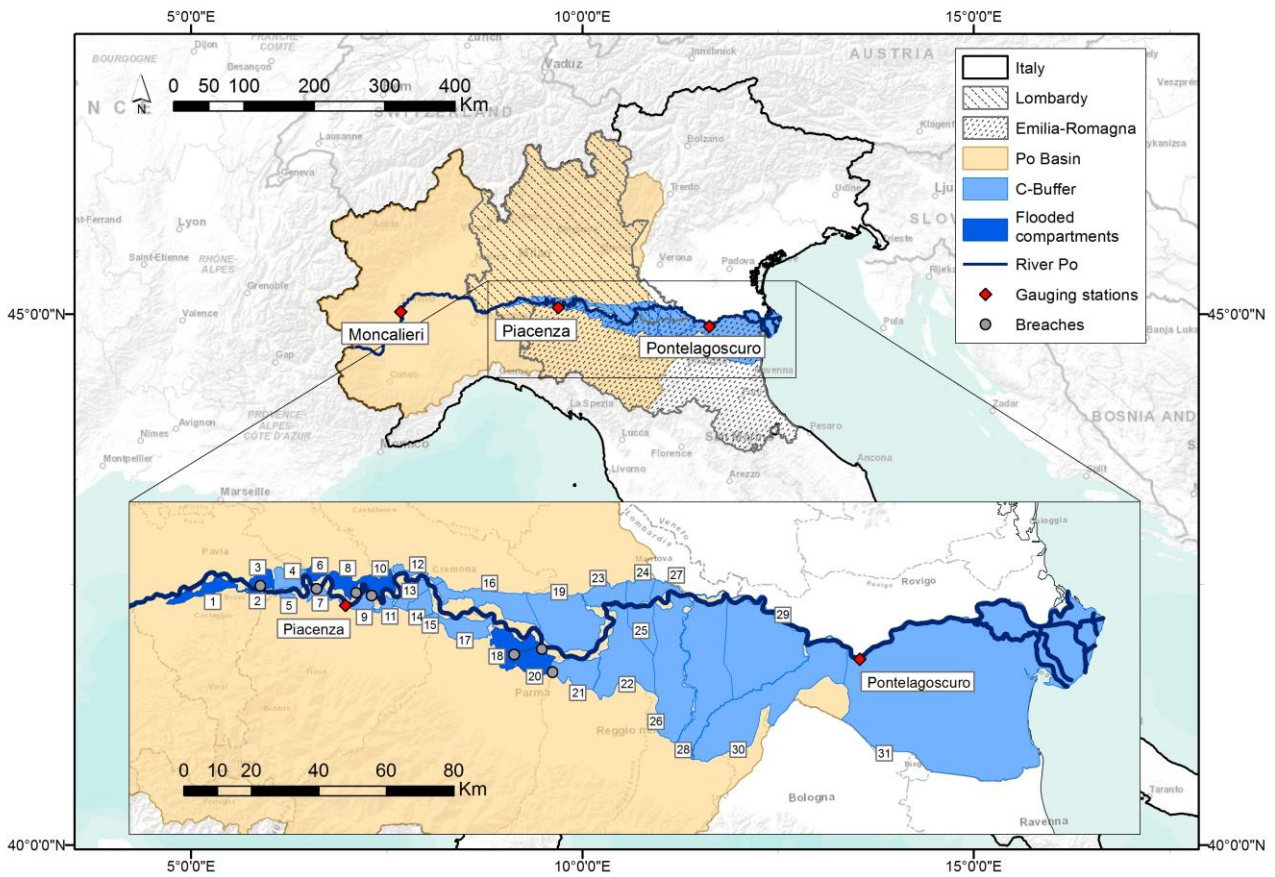
**Table 6.** Flood inundation of C-Buffer area for the Tr500 event. Inundation characteristics simulated by the quasi-2D model in each flooded compartments (see also Figure 5).

<i>Compartment</i>	<i>Max. water depth <math>W_d</math> [m]</i>	<i>Max. water level <math>F_{el}</math> [m a.s.l.]</i>	<i>Volume [<math>10^6</math> m<sup>3</sup>]</i>	<i>Flooded urban area 1954 <math>A_{tot}</math> [ha]</i>	<i>Flooded urban area 2008 <math>A_{tot}</math> [ha]</i>
1	5.3	58.9	4.58	2.62	3.89
2	10.5	60.7	1.89	15.49	21.74
3	8.8	62.1	135.84	53.12	90.80
6	6.9	55.7	61.19	22.19	31.61
8	8.4	51.3	143.68	112.84	227.04
10	7.1	44.6	81.08	101.88	143.78
18	6.0	29.2	27.29	43.56	92.11
20	5.6	31.5	207.14	144.25	453.23
<i>8 Compartments</i>	-	-	~ 663	~ 496	~ 1064

1024  
1025

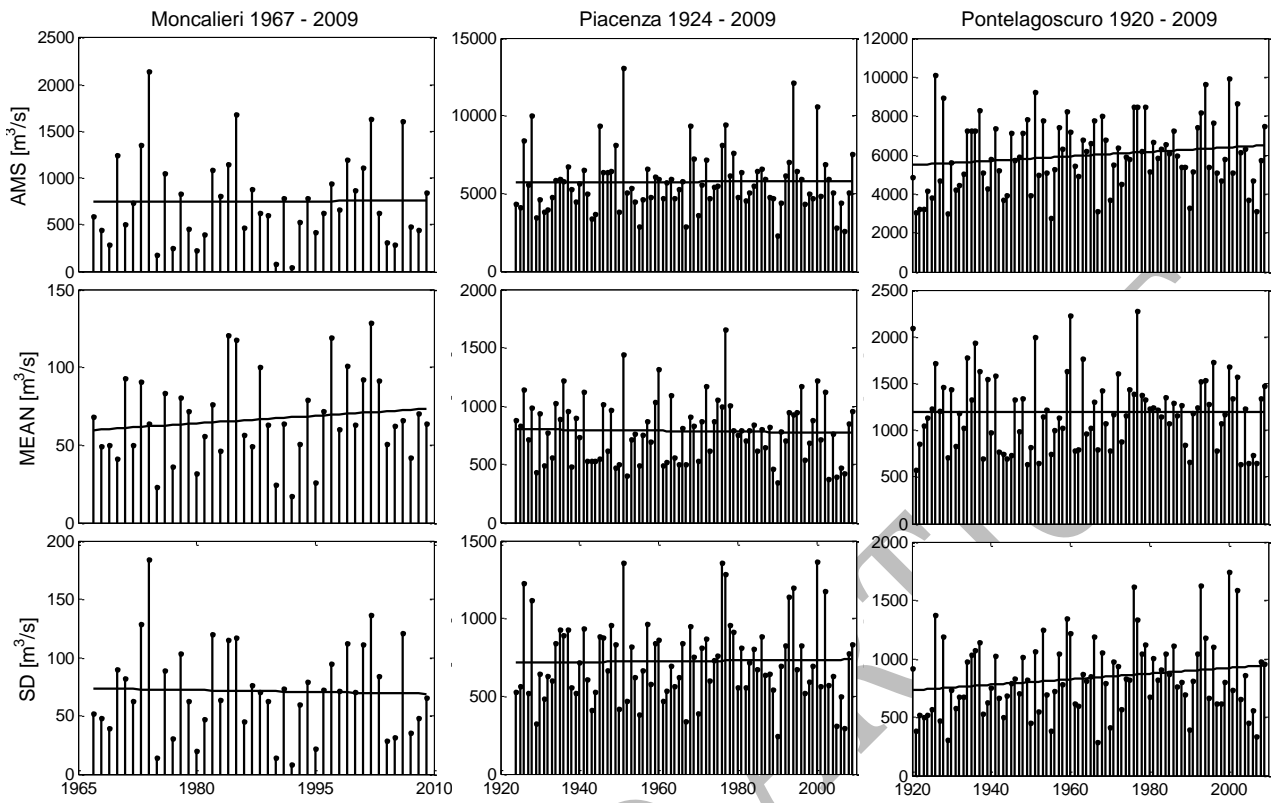
ACCEPTED ARTICLE

1026 **FIGURE**  
1027



1028  
1029 **Fig. 1.** Study area: Po river basin with gauging stations (red dots) and Regions of interests (Emilia-Romagna and  
1030 Lombardy); the numbered compartments (blue polygons) represent the area outside the levee system that is  
1031 exposed to a residual flood risk (i.e. C-Buffer zone; AdB-Po, 1999, Castellarin et al., 2011b).

1032  
1033  
1034  
1035  
1036  
1037  
1038  
1039  
1040



1041

1042

1043

1044

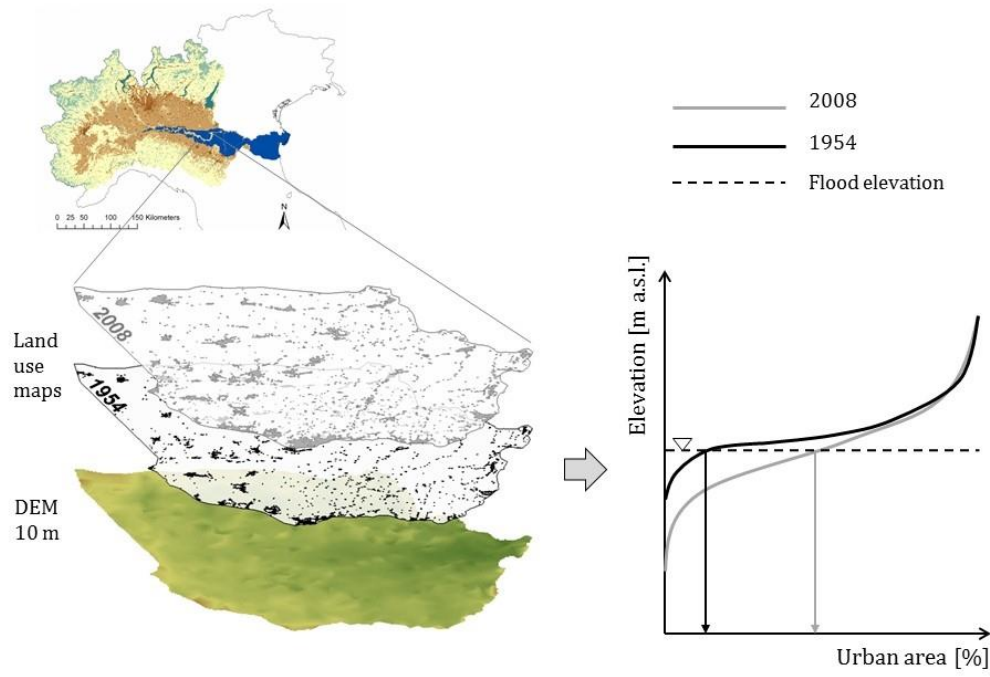
1045

1046

1047

1048

**Figure 2.** Annual series of maxima (AMS), mean (MEAN) and standard deviation (SD) of daily streamflows for Po river at Moncalieri (left), Piacenza (center) and Pontelagoscuro (right).



1049

1050 **Fig. 3.** Examples of Hypsometric Vulnerability Curves for a specific C-Buffer compartment for 1954 and 2008.

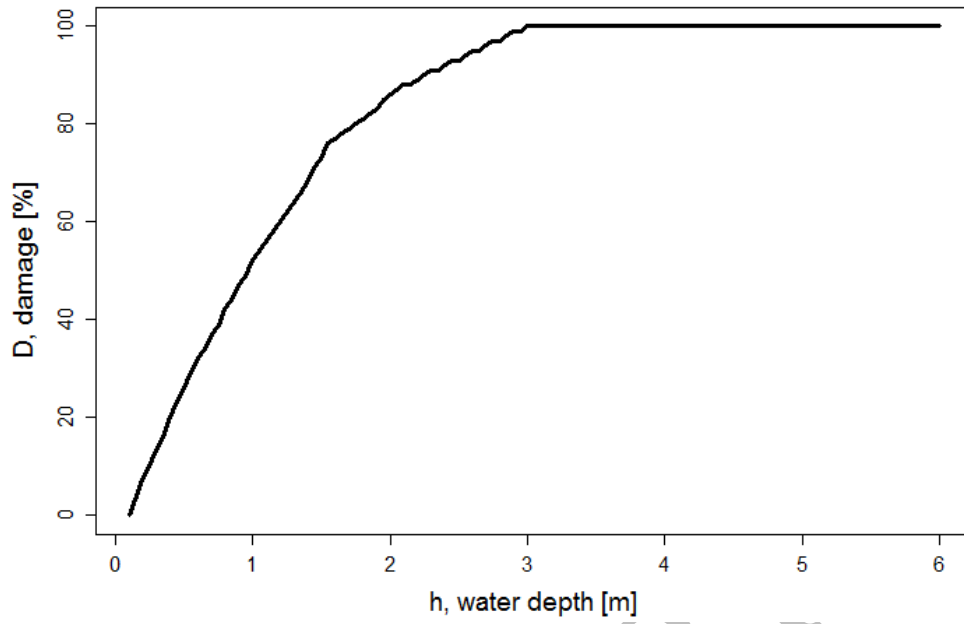
1051

1052

ACCEPTED AUTHOR



1053



1054

1055

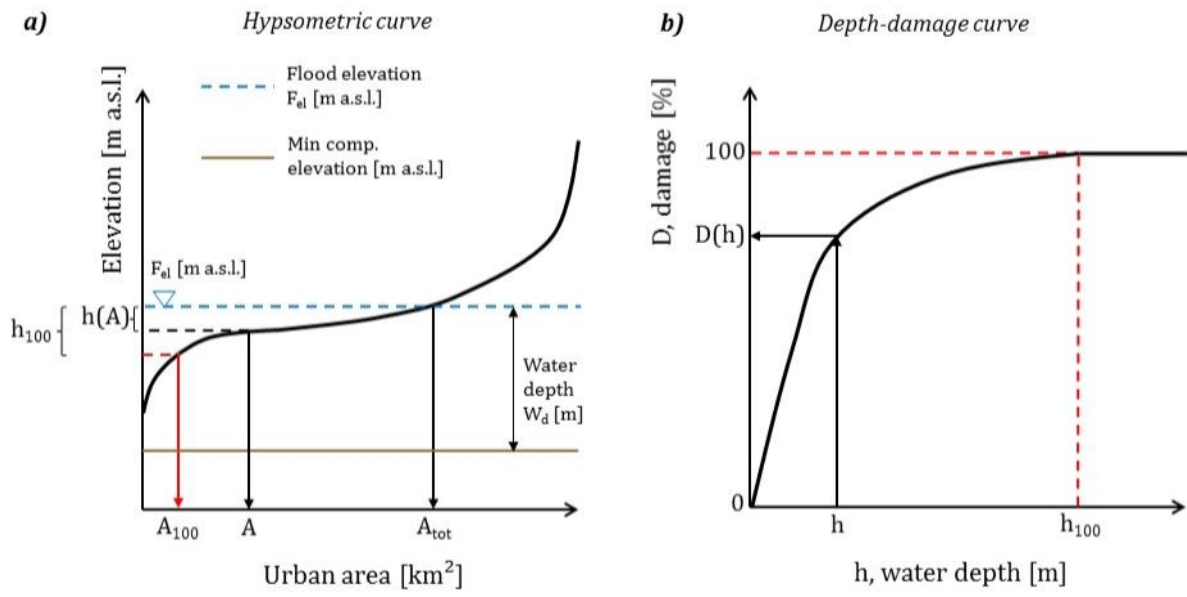
**Fig. 4.** Depth-Damage curve adopted for urban areas and provided by MCM (Penning-Roswell et al., 2010).

1056

ACCEPTED ARTICLE

1057

1058



1059

1060

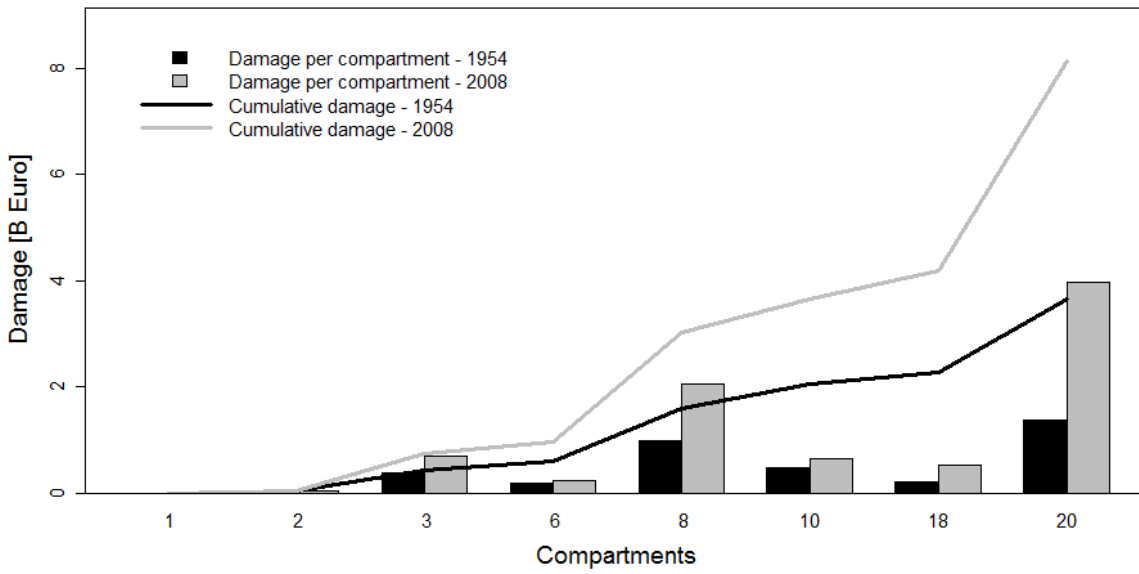
1061

1062

**Fig. 5.** Schematic representation of the combination of a Hypsometric (left) and depth-damage (right) curves for estimating flood damages in urban areas.

ACCEPTED AUTHOR

1063



1064

1065

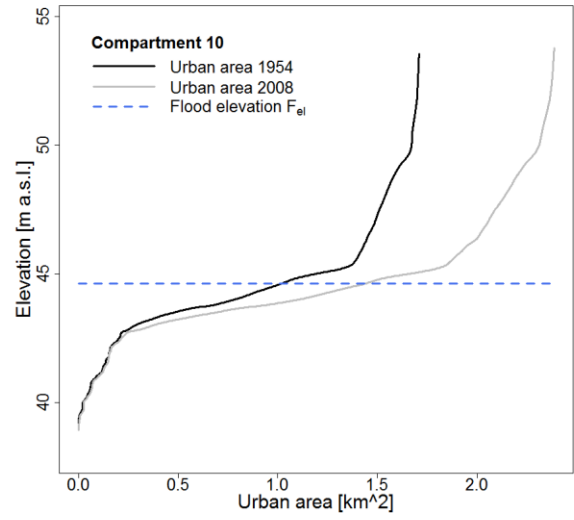
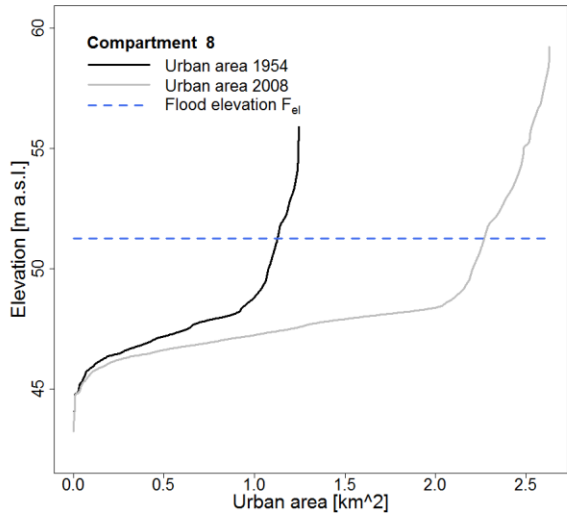
1066

1067

**Figure 6.** Bars indicate the expected economic losses in billions of Euros (left axis) for the C-Buffer zone compartments and the Tr500 event with urban extent of 1954 (black) or 2008 (grey); solid lines (right axis) report the cumulative economic losses from compartment 1 to 20 for 1954 (black) and 2008 (grey).

1068

1069



1070

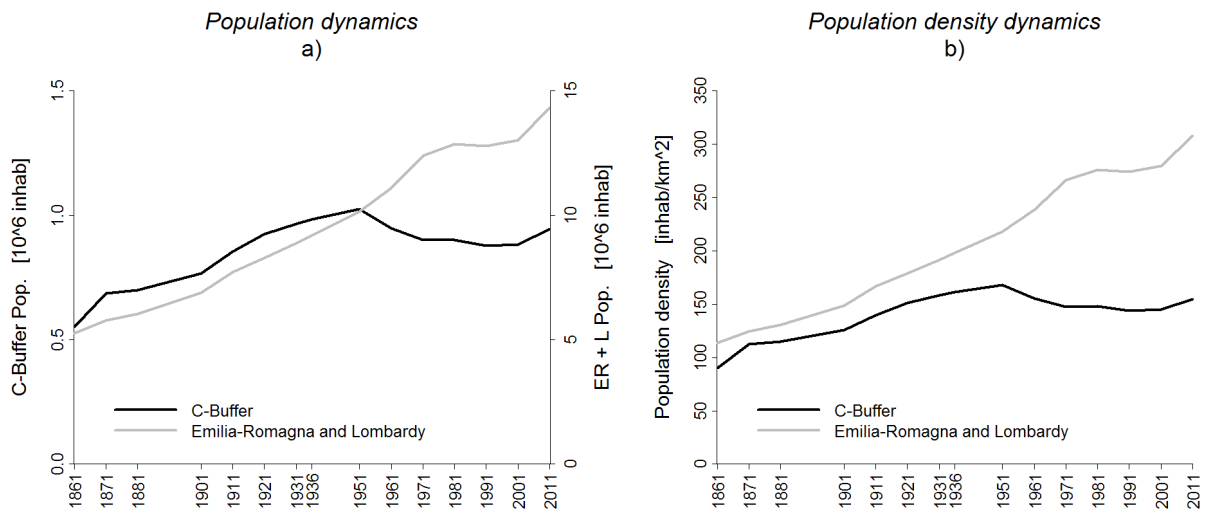
1071

1072

1073

**Figure 7.** Hypsometric Vulnerability Curves (HVCs) expressed in terms of total urban area extent [km<sup>2</sup>] for Compartment 8 (left) and 10 (right) in 1954 (black line) and 2008 (grey line) with the maximum inundation level for the Tr500 event (blue dashed line).

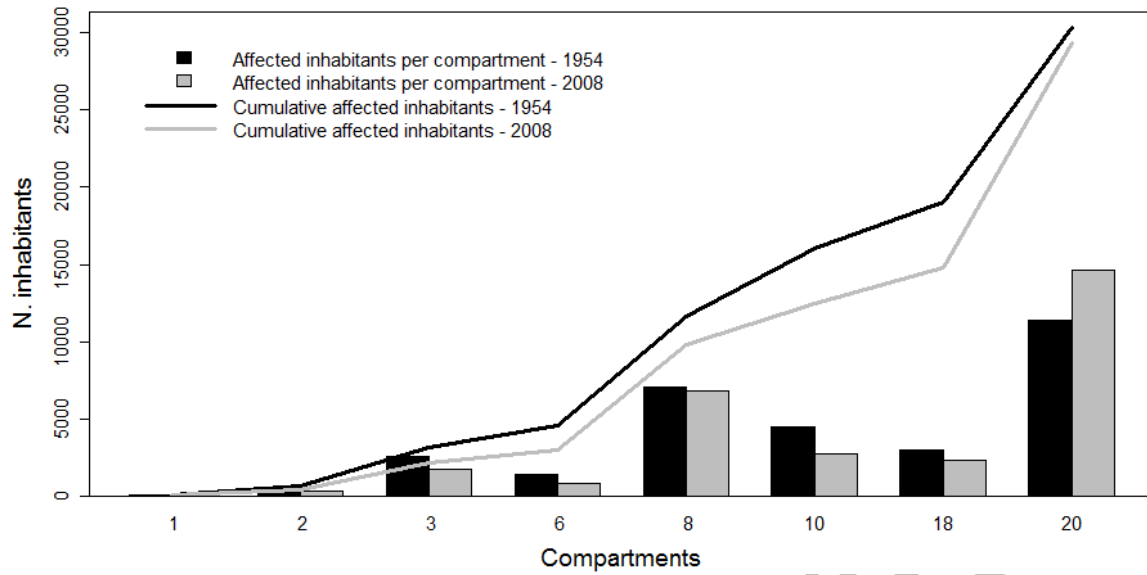
ACCEPTED ARTICLE



1074  
 1075  
 1076  
 1077

**Figure 8.** Demographic dynamics in the main administrative districts of the Po basin (Emilia-Romagna and Lombardy, see Fig. 1, grey line right axis) and in the C-Buffer zone (black line, left axis) in terms of number of inhabitants and population density (panel b).

ACCEPTED ARTICLE



1078

1079

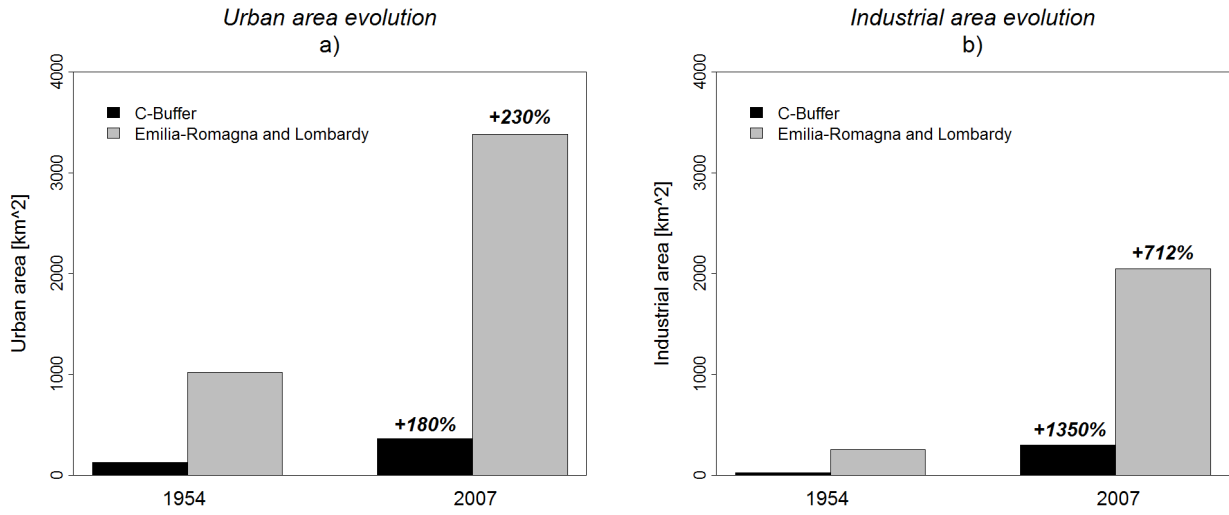
1080

1081

1082

**Figure 9.** Estimated number of inhabitants that are potentially affected by the Tr500 inundation scenario for each flooded C-Buffer compartment (bars) and cumulated moving downstream (lines) considering the population living in the flood-prone area in 1954 (black) and 2008 (grey).

ACCEPTED ARTICLE



1083

1084

1085

**Figure 10.** Evolution over the last half-century of the overall extent of urban (panel a) and industrial (panel b) areas in the C-Buffer (black bars) and in Emilia-Romagna plus Lombardy regions (grey bars).

ACCEPTED ARTICLE